

Neutrino non-standard interactions meet precision measurements of N_{eff}

Yong Du^a and Jiang-Hao Yu^{a,b,c,d,e}

^a*CAS Key Laboratory of Theoretical Physics,
Institute of Theoretical Physics, Chinese Academy of Sciences,
Beijing 100190, P.R. China*

^b*School of Physical Sciences, University of Chinese Academy of Sciences,
Beijing 100049, P.R. China*

^c*Center for High Energy Physics, Peking University,
Beijing 100871, P.R. China*

^d*School of Fundamental Physics and Mathematical Sciences,
Hangzhou Institute for Advanced Study, UCAS,
Hangzhou 310024, P.R. China*

^e*International Centre for Theoretical Physics Asia-Pacific,
Beijing/Hangzhou, P.R. China*

E-mail: yongdu@itp.ac.cn, jhyu@itp.ac.cn

ABSTRACT: The number of relativistic species, N_{eff} , has been precisely calculated in the standard model, and would be measured to the percent level by CMB-S4 in future. Neutral-current non-standard interactions would affect neutrino decoupling in the early Universe, thus modifying N_{eff} . We parameterize those operators up to dimension-7 in the effective field theory framework, and then provide a complete, generic and analytical dictionary for the collision term integrals. From precision measurements of N_{eff} , the most stringent constraint is obtained for the dimension-6 vector-type neutrino-electron operator, whose scale is constrained to be above about 195 (331) GeV from Planck (CMB-S4). We find our results complementary to other experiments like neutrino coherent scattering, neutrino oscillation, collider, and neutrino deep inelastic scattering experiments.

KEYWORDS: Beyond Standard Model, Cosmology of Theories beyond the SM, Effective Field Theories, Neutrino Physics

ARXIV EPRINT: [2101.10475](https://arxiv.org/abs/2101.10475)

Contents

1	Introduction	1
2	Brief review of neutrino decoupling and N_{eff}	4
3	Setup of the Boltzmann equation	5
3.1	The Boltzmann equation	5
3.1.1	Evolution of T_γ , T_ν and μ_ν in the SM	6
3.2	Brief review of the collision term integrals	6
4	EFT operators and the collision term integrals	9
4.1	List of relevant EFT operators	9
4.2	Choices of the independent bases	12
4.3	Corrections from m_e , spin statistics and chemical potentials	14
4.4	A complete generic and analytical dictionary of the collision term integrals	14
4.4.1	$\langle \mathcal{M}^2 \rangle_{1+2 \rightarrow 3+4} = 1$	15
4.4.2	$\langle \mathcal{M}^2 \rangle_{1+2 \rightarrow 3+4} = p_{ij}$	15
4.4.3	$\langle \mathcal{M}^2 \rangle_{1+2 \rightarrow 3+4} = p_{ij} \cdot p_{mn}$	16
4.4.4	$\langle \mathcal{M}^2 \rangle_{1+2 \rightarrow 3+4} = p_{ij} \cdot p_{mn} \cdot p_{st}$	16
5	Constraints on EFT operators from N_{eff}	18
5.1	Constraints on Λ with fixed Wilson coefficients	19
5.2	Constraints on Wilson coefficients with fixed Λ	22
5.3	Comparison with current constraints on NC NSIs	24
6	Conclusions	27

1 Introduction

The great triumph of the Standard Model (SM) of particle physics was the discovery of the Higgs particle in 2012 [1, 2]. However, SM can not be the complete theory as there are still several unsolved puzzles, such as neutrino masses, dark matter and baryon asymmetry of the Universe, which require new physics beyond the SM. Tremendous new physics models have been invented and studied to address these issues, yet no definite signals of any of these models have been observed at colliders or from low-energy precision measurements. This has in turn motivated physicists to search for new physics in a model-independent and systematic way.

Effective Field Theories (EFTs) provide such a systematic and model-independent framework for the study of new physics, especially if its characteristic scale is above the weak scale. The EFT, obtained by integrating out the newly introduced heavy particles to

the SM, is called the SM EFT (SMEFT) [3–11], which respects the SM gauge group and is valid until down to the weak scale. Below the weak scale, the corresponding EFT is the Low-energy EFT (LEFT) [12–15], where the top quark, the SU(2) gauge bosons and the Higgs particle of the SMEFT are all integrated out. As a consequence, the Lagrangian of the LEFT respects the $SU(3)_c \times U(1)_{EM}$ gauge group.

Since the discovery of neutrino oscillations [16–21], neutrino non-standard interactions (NSIs), firstly discussed in refs. [22, 23] and nicely reviewed in refs. [24–28], have gained significant attention in recent years and can be described by the LEFT framework. Very stringent constraints on these NSI operators have been obtained, see, for example, refs. [29–43] for recent theoretical studies and refs. [44–48] for experimental investigation. On the other hand, since these NSI operators can be matched to SMEFT operators, constraints on the NSIs from low-energy experiments can also be translated into constraints on the SMEFT operators, thus also on the UV models. While we are not interested in UV completion of neutrino NSIs in this work, we comment that these NSI operators can be induced, for example, from the leptoquark model [49] and/or the $U(1)'$ models, see, for example, the discussion in ref. [50].

These neutrino NSI operators can be generically classified into charge-current (CC) and neutral-current (NC) ones.¹ In ref. [56], bounds on the CC NSIs were obtained from the Cabibbo-Kobayashi-Maskawa (CKM) [57, 58] unitarity, weak universality tests from pion decay [59], short-baseline neutrino oscillation experiments KARMEN [60] and NOMAD [61, 62], and loop corrections to $\mu \rightarrow e$ conversion in gold [63]. Very recently, CC NSIs were studied in refs. [64, 65] within the SMEFT framework.

For NC NSIs at dimension-6, one-loop electroweak radiative corrections was recently calculated in ref. [66] within the SM, including two-loop matching and three-loop running for the lepton sector. Constraints from collider searches, dark matter direct detection experiments, and superbeam experiments can be found in refs. [67–81]. See refs. [53, 82–85] for neutrino trident production and neutrino-electron scattering from DUNE, refs. [24, 56, 86–93] for oscillation experiments, refs. [24, 94] for loop bounds on dimension-6 electron-neutrino contact operators, refs. [38, 95–101] for neutrino coherent scattering experiments, and ref. [102] for FASER ν . Note also that the dimension-6 NC electron self-interacting NSIs could modify the weak mixing angle. This angle would be very precisely measured by the upcoming low-energy MOLLER experiment at the Jefferson Lab [103] and the planned P2 experiment at MESA [104]. Recently, SM prediction of the weak mixing angle at two-loop has been obtained in ref. [105]. For NC neutrino NSIs up to dimension-7, part of them was previously investigated in refs. [51, 75, 106–112], while a relatively more comprehensive study was recently presented in ref. [38].

However, not all NC NSI operators up to dimension-7 are bounded from ref. [38] or existing work. For example, dimension-6 neutrino self-interacting operators are not studied, since previous work mainly focuses on neutrino oscillation, neutrino coherent scattering and collider experiments etc., which are insensitive to these operators. Furthermore, at dimension-7, only neutrino-photon, neutrino-gluon, and neutrino-quark operators are in-

¹In the case of generic neutrino interactions, see refs. [51–55].

investigated [38], while the dimension-7 neutrino-electron operators are not yet considered to be constrained.

In the early Universe where only neutrinos, electrons, positrons, and photons are present, these neutrino-neutrino, neutrino-electron/positron and neutrino-photon NC NSIs would affect neutrino decoupling, thus modifying the effective number of relativistic degrees of freedom, viz., N_{eff} . In light of the precision measurements of N_{eff} from LEP [113] and Planck [114], the upcoming SPT-3G [115] and the Simons Observatory [116], as well as the proposal from Cosmic Microwave Background-Stage 4 (CMB-S4) [117], CORE [118], PICO [119] and CMB-HD [120], one naturally expects constraints on these NC NSIs from N_{eff} .

In this work, we investigate all kinds of neutrino-neutrino, neutrino-electron/positron and neutrino-photon NC NSI operators up to dimension-7, as well as their impact on N_{eff} . Since the light mediator directly serves as one additional degree of freedom and thus resulting in large N_{eff} , these NC NSI operators we consider in this work are assumed to be induced by integrating out some heavy new physics above $\sim \mathcal{O}(100 \text{ MeV})$ that is about the muon mass or heavier.

To obtain new physics corrections to N_{eff} , the SM prediction to N_{eff} has to be known precisely in the first place. However, it has been known for a long time that the precision calculation of N_{eff} is very challenging. Within the SM, the precision calculation of N_{eff} has been carried out through the density matrix formalism. Due to its complexity, however, the density matrix formalism is very difficult to generalize to other scenarios, for example, when new physics is present. For recent development of precision calculation of N_{eff} , see refs. [121–125].

In this work, we adopt the strategy developed in refs. [124, 125] that reproduces the SM prediction of N_{eff} , works fast, and can be easily generalized to include effects from various new physics. To find corrections to N_{eff} from some new physics, this strategy has already been applied in refs. [126, 127] with the introduction of right-handed partners of neutrinos, refs. [128, 129] with dark matter and/or sterile neutrinos, ref. [130] for dark photon, ref. [131] with the introduction of neutrino-scalar interactions, ref. [132] with the inclusion of neutrino flavor oscillation and primordial nucleosynthesis, and ref. [133] with a light Z' to explain the recent XENON1T excess [134]. Applying this strategy to the calculation of N_{eff} with the inclusion of NC NSIs up to dimension-7, in this work, we

- provide a complete, generic and analytical dictionary for the collision term integrals in section 4. This dictionary can be used directly for computing corrections to N_{eff} from some new physics, either in the EFT framework up to dimension-7, or in some UV models as long as the new physics is above $\sim \mathcal{O}(100 \text{ MeV})$;
- present our constraints on the NC neutrino NSI operators up to dimension-7 in section 5, and also compare our results with previous ones.

The rest of this work is organized as follows. We briefly review neutrino decoupling in the early Universe and the definition of N_{eff} in section 2. In section 3, we discuss the strategy developed in refs. [124, 125], and then summarize our strategy for calculating

the collision terms integrals. Since these collision term integrals are essential to boost the calculation of N_{eff} , we provide a complete generic and analytical dictionary of the collision term integrals, as well as the NSI operators we study in this work in section 4. Constraints on these NC NSI operators are presented in section 5. We conclude in section 6.

2 Brief review of neutrino decoupling and N_{eff}

In the early Universe when the temperature is above $\mathcal{O}(10)$ MeV and below the muon mass, electrons, positrons, neutrinos and photons are in thermal equilibrium from electroweak interactions. As the Universe expands and the temperature cools down, neutrinos decouple from the rest of the plasma at around $T_{\text{dec}} = 2$ MeV. The neutrinos then undergo simple dilution from the expansion of the Universe, while e^\pm and photons are still in thermal equilibrium. However, when the photon temperature cools further down below the electron mass m_e , $\gamma\gamma \rightarrow e^+e^-$ becomes suppressed while the inverse process is still permitted, heating up the photons.

The number of relativistic degrees of freedom during this period can be parameterized by N_{eff} [135–137]:

$$\rho_R = \left[1 + \frac{7}{8} \left(\frac{4}{11} \right)^{\frac{4}{3}} N_{\text{eff}} \right] \rho_\gamma \tag{2.1}$$

with ρ_γ the photon energy density, and ρ_R the total energy density from all relativistic species during this epoch. Equivalently,

$$N_{\text{eff}} \equiv \left(\frac{\rho_R - \rho_\gamma}{\rho_\nu^0} \right) \left(\frac{\rho_\gamma^0}{\rho_\gamma} \right), \tag{2.2}$$

with ρ_ν^0 the energy density of a single massless neutrino, and ρ_γ^0 the energy density of photons in the instantaneous decoupling limit. Obviously, in the instantaneous limit, $\rho_\gamma^0 = \rho_\gamma$ and $\rho_R = 3\rho_\nu^0 + \rho_\gamma$, resulting in the well-known $N_{\text{eff}} = 3$.

On the other hand, due to the tininess of neutrino masses, the three flavor neutrinos can be effectively taken as massless, permitting to express N_{eff} in eq. (2.2) also in terms of the photon temperature T_γ and the neutrino temperature T_ν as, upon assuming $T_\gamma = T_e$ which is valid since photons and electrons are tightly coupled during neutrino decoupling,

$$N_{\text{eff}} = 3 \left(\frac{11}{4} \right)^{4/3} \left(\frac{T_\nu}{T_\gamma} \right)^4. \tag{2.3}$$

Similarly, in the instantaneous decoupling limit, $T_\nu/T_\gamma = (4/11)^{1/3}$ [138] and once again $N_{\text{eff}} = 3$.

However, it has been known for decades that the instantaneous decoupling picture is not accurate. Indeed, neutrinos are still slightly interacting with the electromagnetic plasma, and neutrino oscillations are also active during neutrino decoupling [139–142]. Furthermore, the electromagnetic plasma also receives corrections from finite temperature QED corrections. Taking all these effects into account, one finds $N_{\text{eff}} = 3.044$ [123, 132]. Corrections from these effects will be discussed further in detail in sections 3.1.1 and 4.3.

3 Setup of the Boltzmann equation

Evolution of phase space distribution (PSD) of any particle in the early Universe is governed by the Boltzmann equation, which we briefly review in this subsection. As mentioned in the introduction, we follow the discussion in ref. [125], which simplifies the calculation of N_{eff} significantly and reproduces the prediction for N_{eff} by using the density matrix formalism.

3.1 The Boltzmann equation

The Boltzmann equation reads

$$\frac{\partial f_i}{\partial t} - Hp \frac{\partial f_i}{\partial p} = \mathcal{C}[f_i], \quad (3.1)$$

with $f_i(p, t)$ the PSD for particle i , H the Planck constant that accounts for the dilution effect from the expansion of the Universe, and \mathcal{C} the collision term defined as²

$$\begin{aligned} \mathcal{C}[f_i] \equiv & \frac{1}{2E_i} \sum_{X,Y} \int \prod_{i,j} d\Pi_{X_i} d\Pi_{Y_j} (2\pi)^4 \delta^4(p_i + p_X - p_Y) \\ & \times \left(\langle \mathcal{M}^2 \rangle_{Y \rightarrow i+X} \prod_{i,j} f_{Y_j} [1 \pm f_i] [1 \pm f_{X_i}] - \langle \mathcal{M}^2 \rangle_{i+X \rightarrow Y} \prod_{i,j} f_i f_{X_i} [1 \pm f_{Y_j}] \right), \end{aligned} \quad (3.2)$$

where $d\Pi_i \equiv d^3p_i / [(2\pi)^3 2E_i]$ and “+ (−)” is for bosonic (fermionic) particles. Note that the difference in the last line above correctly accounts for the production and annihilation of particle i .

Upon integrating over the phase space of particle i on both sides of eq. (3.1), one finds³

$$\frac{dn}{dt} + 3Hn = \frac{\delta n}{\delta t} \equiv \int g \frac{d^3p}{(2\pi)^3} \mathcal{C}[f], \quad (3.3)$$

$$\frac{d\rho}{dt} + 3H(\rho + p) = \frac{\delta \rho}{\delta t} \equiv \int gE \frac{d^3p}{(2\pi)^3} \mathcal{C}[f], \quad (3.4)$$

where g is the intrinsic degree of freedom of particle i , E is its energy, and n and ρ are the number and the energy densities of particle i respectively. Note that after the phase space integration on the right hand side of eqs. (3.3)–(3.4), $\delta n/\delta t$ and $\delta \rho/\delta t$ are functions of the temperature T , the chemical potential μ and the model parameters only.⁴ Thus, in terms of the Hubble parameter, one can readily obtain the following equations through the application of the chain rule:

$$\frac{dT}{dt} = \frac{1}{\frac{\partial n}{\partial \mu} \frac{\partial \rho}{\partial T} - \frac{\partial n}{\partial T} \frac{\partial \rho}{\partial \mu}} \left[-3H \left((p + \rho) \frac{\partial n}{\partial \mu} - n \frac{\partial \rho}{\partial \mu} \right) + \frac{\partial n}{\partial \mu} \frac{\delta \rho}{\delta t} - \frac{\partial \rho}{\partial \mu} \frac{\delta n}{\delta t} \right] \quad (3.5)$$

$$\frac{d\mu}{dt} = \frac{-1}{\frac{\partial n}{\partial \mu} \frac{\partial \rho}{\partial T} - \frac{\partial n}{\partial T} \frac{\partial \rho}{\partial \mu}} \left[-3H \left((p + \rho) \frac{\partial n}{\partial T} - n \frac{\partial \rho}{\partial T} \right) + \frac{\partial n}{\partial T} \frac{\delta \rho}{\delta t} - \frac{\partial \rho}{\partial T} \frac{\delta n}{\delta t} \right]. \quad (3.6)$$

²Note that in our setup, we include the symmetry factor in the definition of $\langle \mathcal{M}^2 \rangle$ throughout this work.

³Without any ambiguity, we suppress the index i starting from here.

⁴With the inclusion of NSI operators, it will also depend on the scale of new physics and the Wilson coefficients.

These two equations effectively describe the evolution of T and μ for any particles in the early Universe, and can thus be used to solve the decoupling of neutrinos from the rest of the plasma as we will see later in this section.

3.1.1 Evolution of T_γ , T_ν and μ_ν in the SM

At the time of neutrino decoupling, since photons and electrons are still tightly coupled, one can safely set $\mu_\gamma = \mu_e = 0$ and $T_\gamma = T_e$. By applying eqs. (3.5)–(3.6), one obtains [125]

$$\frac{dT_\gamma}{dt} = -\frac{4H\rho_\gamma + 3H(\rho_e + p_e) + \frac{\delta\rho_{\nu e}}{\delta t} + \frac{\delta\rho_{\nu\mu}}{\delta t} + \frac{\delta\rho_{\nu\tau}}{\delta t}}{\frac{\partial\rho_\gamma}{\partial T_\gamma} + \frac{\partial\rho_e}{\partial T_\gamma}}, \quad (3.7)$$

$$\frac{dT_{\nu\alpha}}{dt} = -HT_{\nu\alpha} + \frac{\delta\rho_{\nu\alpha}}{\delta t} / \frac{\partial\rho_{\nu\alpha}}{\partial T_{\nu\alpha}}, \quad \alpha = e, \mu, \tau. \quad (3.8)$$

Note that the above equation for T_γ is derived assuming the finite temperature corrections are negligible, while it has been known for a long time that this is not the case especially given the precision measurements of N_{eff} from future experiments. To be clearer, in the future, N_{eff} will be measured to the percent level, while finite temperature corrections to N_{eff} is also at the percent level [117–120, 143–146]. Therefore, to correctly interpret the results from future experiments and/or to disentangle contributions to N_{eff} from any potential new physics from the SM, the QED corrections have to be included.

The leading-order QED corrections were obtained decades ago [147, 148], and higher-order corrections up to $\mathcal{O}(e^4)$ were recently calculated in ref. [121], where the authors found corrections to N_{eff} are about -0.0009 and 10^{-6} at $\mathcal{O}(e^3)$ and $\mathcal{O}(e^4)$ respectively. Since both corrections at $\mathcal{O}(e^3)$ and $\mathcal{O}(e^4)$ exceed the proposed precision target of the future experiments, we neglect those in our setup and only keep the finite temperature corrections up to $\mathcal{O}(e^2)$. On the other hand, neutrino oscillations also lead to a correction to N_{eff} , which is about 0.0007 as reported in refs. [139, 140, 149]. Note that, as was pointed out in ref. [121], since contributions to N_{eff} from neutrino oscillations and the finite temperature corrections at $\mathcal{O}(e^3)$ are comparable, they shall both be included for a consistent precision calculation of N_{eff} . However, as stated above, due to their smallness, we also neglect contributions from neutrino oscillations in this work.

To conclude this subsection, we show the result for T_γ with the inclusion of the aforementioned finite temperature corrections following the notations of refs. [121, 125]:

$$\frac{dT_\gamma}{dt} = -\frac{4H\rho_\gamma + 3H(\rho_e + p_e) + 3HT_\gamma \frac{dP_{\text{int}}}{dT_\gamma} + \frac{\delta\rho_{\nu e}}{\delta t} + \frac{\delta\rho_{\nu\mu}}{\delta t} + \frac{\delta\rho_{\nu\tau}}{\delta t}}{\frac{\partial\rho_\gamma}{\partial T_\gamma} + \frac{\partial\rho_e}{\partial T_\gamma} + T_\gamma \frac{d^2P_{\text{int}}}{dT_\gamma^2}}, \quad (3.9)$$

where P_{int} and $\rho_{\text{int}} \equiv -P_{\text{int}} + dP_{\text{int}}/d\ln T_\gamma$ are finite temperature corrections to the electromagnetic pressure and the electromagnetic energy density respectively, whose analytical expressions can be found in ref. [121].

3.2 Brief review of the collision term integrals

From eqs. (3.9) and (3.8), one can then solve $T_\gamma(t)$ and $T_\nu(t)$, and thus N_{eff} at the time of neutrino decoupling. From eqs. (3.3)–(3.4), we conclude that to solve $T_\gamma(t)$ and $T_\nu(t)$,

the remaining task is to first finish these phase space integrals, which are in general very challenging with no analytical expressions. This in turn slows down numerical calculation of N_{eff} , especially in the presence of new physics. However, as pointed out in ref. [125], analytical results for those collision term integrals exist in the Maxwell-Boltzmann limit, as a result, numerical calculation of N_{eff} can be boosted significantly. For specific processes in the SM, the author of refs. [125] presented analytical results for the collision terms integrals in ref. [124], which, however, can not be generalized to processes in the presence of new physics. In light of this, and since the analytical forms of the collision term integrals are essential to boost the numerical calculation of N_{eff} , we present a full generic and analytical dictionary for the collision term integrals in section 4, while present the method we use to obtain these collision term integrals in this subsection.

To start, we consider the collision term integrals for $2 \rightarrow 2$ processes as these are the only interaction types relevant for N_{eff} calculation in the SM and with the inclusion of NSI operators considered in this work.⁵ Upon leaving out the irrelevant factor g , for a generic process $1 + 2 \rightarrow 3 + 4$, one can write the collision term integrals on the right hand of eqs. (3.3)–(3.4) generically as

$$C^{(j)} \equiv \int E_1^j \frac{d^3 p_1}{(2\pi)^3} \mathcal{C}[f_1] \quad \Leftrightarrow \quad \begin{cases} j = 0, & \text{for number density} \\ j = 1, & \text{for energy density} \end{cases}, \quad (3.10)$$

with p_i and E_i the four-momentum and the energy of the i -th particle. To simplify the collision term integral, we reproduce the results presented in appendix D of ref. [161] and cite the result here:⁶

$$C^{(j)} = \frac{1}{2(2\pi)^6} \int E_1^j dE_1 dE_2 dE_3 \cdot (|\vec{p}_1| |\vec{p}_2| |\vec{p}_3|) \cdot \Theta \left(Q + |\vec{p}_1|^2 + |\vec{p}_2|^2 + |\vec{p}_3|^2 + 2\gamma \right) \\ \times \left(\int_{\max(-1, \cos \theta_-)}^{\min(1, \cos \theta_+)} d(\cos \theta) \int_{\cos \alpha_-}^{\cos \alpha_+} d(\cos \alpha) \frac{\langle \mathcal{M}^2 \rangle_{1+2 \rightarrow 3+4}}{\sqrt{a \cos^2 \alpha + b \cos \alpha + c}} \right. \\ \left. \times [f_3 f_4 (1 \pm f_1)(1 \pm f_2) - f_1 f_2 (1 \pm f_3)(1 \pm f_4)] \right) \Bigg|_{p_4 \rightarrow p_1 + p_2 - p_3}, \quad (3.11)$$

where α (θ) is the angle between \vec{p}_1 and \vec{p}_2 (\vec{p}_3), and we define

$$Q \equiv m_1^2 + m_2^2 + m_3^2 - m_4^2, \quad (3.12)$$

$$\gamma \equiv E_1 E_2 - E_1 E_3 - E_2 E_3, \quad (3.13)$$

$$\omega \equiv Q + 2\gamma + 2|\vec{p}_1| |\vec{p}_1| \cos \theta, \quad (3.14)$$

$$a \equiv -4|\vec{p}_2|^2 \left(|\vec{p}_1|^2 + |\vec{p}_3|^2 - 2|\vec{p}_1| |\vec{p}_3| \cos \theta \right), \quad (3.15)$$

$$b \equiv 4|\vec{p}_2| \left(|\vec{p}_1| - |\vec{p}_3| \cos \theta \right) \omega, \quad (3.16)$$

$$c \equiv 4|\vec{p}_2|^2 |\vec{p}_3|^2 \sin^2 \theta - \omega^2. \quad (3.17)$$

⁵For decay or inverse decay, the collision term integral, defined is eq. (3.10) is a nine-fold one that can be reduced to a two-fold integral. There are many literatures in the past discussing the collision term integral, see, for example, refs. [121, 137, 139, 140, 149–160].

⁶We assume CP conservation that allows the factorization of $\langle \mathcal{M}^2 \rangle_{1+2 \rightarrow 3+4}$, which is a well-justified approximation for our purpose here.

Note that $a \leq 0$ from above definition, and the integrating regions for α and θ are altered, where

$$\cos \alpha_{\pm} = \frac{-b \mp \sqrt{b^2 - 4ac}}{2a}, \quad (3.18)$$

$$\cos \theta_{\pm} = -\frac{Q + 2|\vec{p}_2|^2 + 2\gamma \mp 2|\vec{p}_2| \sqrt{Q + |\vec{p}_1|^2 + |\vec{p}_2|^2 + |\vec{p}_3|^2 + 2\gamma}}{2|\vec{p}_1||\vec{p}_3|}, \quad (3.19)$$

resulting from the requirement of the existence of physical solutions to the collision term integral. Note also that $\langle \mathcal{M}^2 \rangle_{1+2 \rightarrow 3+4}$ is in general a function of p_{ij} , defined as

$$p_{ij} \equiv p_i \cdot p_j, \quad (i, j = 1, \dots, 4), \quad (3.20)$$

which also depends on the angles α and θ , making the integral in eq. (3.11) too cumbersome to be completed.

Surprisingly, one huge simplification that eventually allows the completion of the integral in eq. (3.11) can be realized when (1) all the particles involved are massless, i.e., $m_i = 0$ ($i = 1, \dots, 4$), leading to

$$Q = 0, \quad \min(1, \cos \theta_+) = 1 = \cos \theta_+, \quad (3.21)$$

and (2) all the particles obey the Maxwell-Boltzmann distribution, permitting analytical expressions for almost all possible forms of $\langle \mathcal{M}^2 \rangle_{1+2 \rightarrow 3+4}$. The only exception is when there exists a light mediator in the t and/or the u channels, where it has been well-known that IR divergence emerges when all external particles become massless, the Compton scattering for example.⁷ However, this IR divergence has to cancel out for any sufficiently inclusive quantities, as is guaranteed by the Kinoshita-Lee-Nauenberg (KLN) theorem [162, 163]. Recently, it is also shown in ref. [164] that to have IR finiteness, one does not necessarily need to sum over both the initial and the final states as stated by the KLN theorem, rather, one only needs to sum over all possible final (initial) state for a given fixed initial (final) state, as long as the forward scattering is also included.

In this work, since we are interested in constraints on new physics from N_{eff} in a model independent manner within the EFT framework, we will mainly focus on scenarios with heavy mediators such that the IR divergence issue mentioned above never shows up. The only exception is the dimension-5 neutrino magnetic dipole operator, which we will discuss in section 4. Furthermore, in order to obtain analytical results, as discussed in last paragraph, we assume all particles (1) are massless, and (2) obey the Maxwell-Boltzmann distribution only when calculating the collision term integrals from eq. (3.11). We then present a complete dictionary for all possible $\langle \mathcal{M}^2 \rangle_{1+2 \rightarrow 3+4}$ up to products with three p_{ij} in $\langle \mathcal{M}^2 \rangle_{1+2 \rightarrow 3+4}$ in section 4, which are also provided in the supplementary material as a **Mathematica** notebook file. Corrections from non-vanishing masses and Fermi-Dirac/Bose-Einstein distribution are also discussed in section 4.

⁷Note, however, that even in the case with a light mediator in the s channel, there is no IR divergence and analytical results for the collision term integrals can always be obtained.

4 EFT operators and the collision term integrals

As no new particles have been observed after the discovery of the Higgs particle in 2012 [1, 165], EFTs have become the natural framework for the study of any new heavy physics. In this work, we are interested in corrections to N_{eff} from higher-dimensional operators in the early Universe. The active degrees of freedom at that time are neutrinos, photons, electrons and positrons. Since the neutrinos decouple from the rest of the plasma at around 2 MeV, for the EFTs to be valid, the potential new physics could be as light as $\sim \mathcal{O}(100 \text{ MeV})$ that is about the muon mass. Note that the lower bound of the new physics scale would also be constrained from, for example, Big Bang Nucleosynthesis. Given that future experiments like CMB-S4 could constrain $\Delta N_{\text{eff}} < 0.06$ at 95% CL [117, 143, 144, 146] with ΔN_{eff} the corrections to SM prediction of N_{eff} , one naturally expects the EFT operators could also be constrained from the precision measurements of N_{eff} .

In this section, we will first enumerate the relevant EFT operators up to dimension-7 in section 4.1. The resulting invariant amplitudes from these operators turn out to be functions of p_{ij} defined in eq. (3.20), model parameters and the Wilson coefficients. Depending on how explicitly the $\langle \mathcal{M}^2 \rangle$ depends on p_{ij} , the collision term integral in eq. (3.11) needs to be calculated case by case. From momentum-energy conservation, the redundancy in collision term integral computation can be reduced to a set of limited number of bases as presented in section 4.2. Starting from these bases, we then present a complete dictionary of the collision term integrals in section 4.4.

4.1 List of relevant EFT operators

We start from the SMEFT, obtained by integrating out the heavy new degrees of freedom introduced to the SM, where the Lagrangian can be expressed as the SM Lagrangian, plus a tower of higher-dimension operators $\mathcal{O}^{(j)}$:

$$\mathcal{L} = \mathcal{L}_{\text{SM}} + \sum_{j \geq 5} \frac{C_j}{\Lambda^{j-4}} \mathcal{O}^{(j)}, \quad (4.1)$$

where C_j 's are the Wilson coefficients and Λ is the characteristic scale of new physics. In this setup, the neutrino masses can be naturally generated through the dimension-5 Weinberg operator [3]. However, for the rest of this work, we neglect the masses of neutrinos due to their tininess compared with the other scales involved in our calculation.

In the early Universe where the active fields are neutrinos, photons, electron and positrons, the Universe can be described by the LEFT, where the top quark, the SU(2) gauge bosons, and the Higgs boson have also been integrated out within the SMEFT, inducing both CC and NC neutrino NSIs. See, for example, ref. [50] for the discussion. However, we point out that CC and NC NSIs are not necessarily generated by heavy particles above the weak scale, instead, it can also be generated by some light particles above the $\mathcal{O}(100 \text{ MeV})$ scale. To illustrate this point, we briefly discuss a toy Z' and a toy pseudo-scalar models here:

- The toy U(1)' model we consider, without restricting ourselves to any other constraints such as anomaly cancellation, collider and cosmological constraints etc., is

Dimensions	Operators	Wilson coefficients
dimension-5	$\mathcal{O}_1^{(5)} = \frac{e}{8\pi^2} (\bar{\nu}_\beta \sigma^{\mu\nu} P_L \nu_\alpha) F_{\mu\nu}$	$C_1^{(5)}$
dimension-6	$\mathcal{O}_{1,f}^{(6)} = (\bar{\nu}_\beta \gamma_\mu P_L \nu_\alpha) (\bar{f} \gamma^\mu f)$	$C_{1,f}^{(6)}$
	$\mathcal{O}_{2,f}^{(6)} = (\bar{\nu}_\beta \gamma_\mu P_L \nu_\alpha) (\bar{f} \gamma^\mu \gamma_5 f)$	$C_{2,f}^{(6)}$
	$\mathcal{O}_3^{(6)} = (\bar{\nu}^c_\beta P_L \nu_\alpha) (\bar{\nu}^c_{\beta'} P_L \nu_{\alpha'}) \clubsuit$	$C_3^{(6)}$
	$\mathcal{O}_4^{(6)} = (\bar{\nu}_\beta \gamma_\mu P_L \nu_\alpha) (\bar{\nu}_{\beta'} \gamma_\mu P_L \nu_{\alpha'}) \clubsuit$	$C_4^{(6)}$
	$\mathcal{O}_5^{(6)} = (\bar{\nu}^c_\beta \sigma^{\mu\nu} P_L \nu_\alpha) (\bar{\nu}^c_{\beta'} \sigma^{\mu\nu} P_L \nu_{\alpha'}) \clubsuit$	$C_5^{(6)}$
dimension-7	$\mathcal{O}_1^{(7)} = \frac{\alpha}{12\pi} (\bar{\nu}^c_\beta P_L \nu_\alpha) F^{\mu\nu} F_{\mu\nu}$	$C_1^{(7)}$
	$\mathcal{O}_2^{(7)} = \frac{\alpha}{8\pi} (\bar{\nu}^c_\beta P_L \nu_\alpha) F^{\mu\nu} \tilde{F}_{\mu\nu}$	$C_2^{(7)}$
	$\mathcal{O}_{5,f}^{(7)} = m_f (\bar{\nu}^c_\beta P_L \nu_\alpha) (\bar{f} f)$	$C_{5,f}^{(7)}$
	$\mathcal{O}_{6,f}^{(7)} = m_f (\bar{\nu}^c_\beta P_L \nu_\alpha) (\bar{f} i \gamma_5 f)$	$C_{6,f}^{(7)}$
	$\mathcal{O}_{7,f}^{(7)} = m_f (\bar{\nu}^c_\beta \sigma^{\mu\nu} P_L \nu_\alpha) (\bar{f} \sigma_{\mu\nu} f)$	$C_{7,f}^{(7)}$
	$\mathcal{O}_{8,f}^{(7)} = (\bar{\nu}^c_{\beta i} \overleftrightarrow{\partial}_\mu P_L \nu_\alpha) (\bar{f} \gamma^\mu f)$	$C_{8,f}^{(7)}$
	$\mathcal{O}_{9,f}^{(7)} = (\bar{\nu}^c_{\beta i} \overleftrightarrow{\partial}_\mu P_L \nu_\alpha) (\bar{f} \gamma^\mu \gamma_5 f)$	$C_{9,f}^{(7)}$
	$\mathcal{O}_{10,f}^{(7)} = \partial_\mu (\bar{\nu}^c_\beta \sigma^{\mu\nu} P_L \nu_\alpha) (\bar{f} \gamma_\nu f)$	$C_{10,f}^{(7)}$
	$\mathcal{O}_{11,f}^{(7)} = \partial_\mu (\bar{\nu}^c_\beta \sigma^{\mu\nu} P_L \nu_\alpha) (\bar{f} \gamma_\nu \gamma_5 f)$	$C_{11,f}^{(7)}$

Table 1. Effective operators relevant for N_{eff} up to dimension-7 with $\alpha, \beta, \alpha', \beta' = e, \mu, \tau$, the neutrino flavor indices, and $f = e$. Operators with \clubsuit 's are the extra operators we consider in this work and the symbol “ c ” along with related operators means charge conjugation. The last column shows our convention for the Wilson coefficients.

the Z' model that can be written as

$$\mathcal{L}_{Z'} = \mathcal{L}_{\text{SM}} - \frac{1}{4} Z'_{\mu\nu} Z'^{\mu\nu} + \frac{1}{2} m_{Z'}^2 Z'_\mu Z'^\mu - g_{Z'} Z'_\mu (\bar{L} \gamma^\mu L + \bar{\ell}_R \gamma^\mu \ell_R), \quad (4.2)$$

where L and ℓ_R are the left-handed lepton doublet and the right-handed lepton singlet under $\text{SU}(2)_L$ respectively, and Z' is the new vector boson charged under the $\text{U}(1)'$ group. For our purpose, Z' needs not to be above the weak scale, and as long as Z'

is above $\sim \mathcal{O}(100 \text{ MeV})$ or equivalently the muon mass, Z' can be integrated out:

$$\begin{aligned} \mathcal{L}_{Z'} \supset & \frac{1}{2} m_{Z'}^2 \left(\frac{g_{Z'}}{p^2 - m_{Z'}^2} \right)^2 \left(\bar{L} \gamma_\mu L + \bar{\ell}_R \gamma_\mu \ell_R \right) \left(\bar{L} \gamma^\mu L + \bar{\ell}_R \gamma^\mu \ell_R \right) \\ & - \frac{g_{Z'}^2}{p^2 - m_{Z'}^2} \left(\bar{L} \gamma^\mu L + \bar{\ell}_R \gamma^\mu \ell_R \right) \left(\bar{L} \gamma^\mu L + \bar{\ell}_R \gamma^\mu \ell_R \right) \\ & \xrightarrow{p^2 \ll m_{Z'}^2} \frac{g_{Z'}^2}{2m_{Z'}^2} \left(\bar{L} \gamma^\mu L + \bar{\ell}_R \gamma^\mu \ell_R \right) \left(\bar{L} \gamma^\mu L + \bar{\ell}_R \gamma^\mu \ell_R \right) + \mathcal{O} \left(\frac{1}{m_{Z'}^4} \right), \end{aligned} \quad (4.3)$$

leading to the NC neutrino-electron and electron-electron contact interactions as seen above when $m_{Z'}$ is larger than the momentum transfer p^2 . During neutrino decoupling, since p^2 is of $\mathcal{O}(10 \text{ MeV})^2$, thus as long as $m_{Z'}$ is above $\mathcal{O}(100 \text{ MeV})$, the EFT after integrating out Z' serves as a good framework for the study of this new physics.

- The toy pseudo-scalar model we consider, without considering any theoretical and/or experimental constraints, can be expressed as

$$\mathcal{L}_{\text{p.s.}} = \mathcal{L}_{\text{SM}} + \frac{1}{2} \partial_\mu \phi \partial^\mu \phi - \frac{1}{2} m_\phi \phi^2 - i g_\phi^{\alpha\beta} \phi \bar{\nu}_\alpha \gamma_5 \nu_\beta, \quad \text{with } \alpha, \beta = e, \mu, \tau, \quad (4.4)$$

where ϕ is the pseudo-scalar with mass m_ϕ . Similarly, as long as m_ϕ is above $\sim \mathcal{O}(100 \text{ MeV})$, one can integrate out the particle ϕ , and obtain the contact neutrino self-interacting operators.

The CC NSIs have been recently studied in refs. [64, 65]. In ref. [65], the authors took the running and the matching effects at different EFT scales into account, and the resulting constraint on the UV scale Λ was found to be as large as about 20 TeV from neutrino oscillation data. The NC operators are the relevant ones for our study in this work, part of which has been previously studied in refs. [51, 75, 107–112], and a comprehensive study was recently presented in ref. [38]. Note that, since the authors in ref. [38] were interested in constraints on these NSIs from neutrino experiments, they did not consider any dimension-6 neutrino self-interacting operators as neutrinos only feebly interact with our matter world. However, since these operators are closely related to N_{eff} by modifying the neutrino number and the energy densities directly through neutrino self-interactions, we include these operators in this work and study constraints on these neutrino self-interacting operators from precision measurements of N_{eff} .⁸ We summarize all the EFT operators up to dimension-7 in table 1 following the notations in ref. [38].

One immediate observation from table 1 is that, the dimension-5 operator in the first row, i.e., the neutrino magnetic dipole operator, corresponds to the light-mediator scenario we discussed at the end of section 3.2. When the intermediate photon shows up in the s -channel, there is no IR divergence, and the collision term integral can be calculated analytically. However, since the intermediate photon can also appear in the t - and/or

⁸Neutrino self-interactions was also proposed to alleviate the Hubble tension between measurements from the Planck [114] and the local groups [166] in ref. [158]. For the most recent work on Hubble tension from neutrino self-interactions, see refs. [167–170].

u -channels for the $\nu_\alpha \nu_\beta \rightarrow \gamma^* \rightarrow \nu_\alpha \nu_\alpha$ ⁹ process for example, the collision term integrals would exhibit the IR divergence discussed earlier. In principle, one could remove this divergence by applying the KLN theorem or following the procedure discussed in ref. [164] for any inclusive observables. However, since the scenario with a light mediator resides in a different regime compared with all the other operators listed in table 1, we leave the light mediator scenario for a future project. We also point out that this operator is very stringently constrained from the magnetic moment of ν_e using Borexino Phase-II solar neutrino data [38, 171], which justifies our ignorance of the $\mathcal{O}_1^{(5)}$ operator for the calculation of N_{eff} . We will discuss more on this in section 5.

Now, including corrections from the dimension-6 and dimension-7 operators in table 1, the invariant amplitude $\langle \mathcal{M}^2 \rangle_{1+2 \rightarrow 3+4}$ in eq. (3.11) can generically be written as:

$$\langle \mathcal{M}^2 \rangle_{1+2 \rightarrow 3+4} = \langle \mathcal{M}_{\text{SM}}^2 + \mathcal{M}_{\text{EFT}}^2 + 2 \text{Re} \mathcal{M}_{\text{SM}} \cdot \mathcal{M}_{\text{EFT}}^\dagger \rangle_{1+2 \rightarrow 3+4}, \quad (4.5)$$

where \mathcal{M}_{SM} and \mathcal{M}_{EFT} are the amplitudes from \mathcal{L}_{SM} and the EFT operators in table 1 respectively. Clearly, when the potential new physics scale Λ is about or above $\mathcal{O}(\Lambda_W)$ with Λ_W the weak scale, the interference term in eq. (4.5) would be of the same order as the SM contributions, and the $\langle \mathcal{M}_{\text{EFT}}^2 \rangle$ term can then be safely neglected.

However, we point out that in the case where $\Lambda \ll \Lambda_W$, though contributions from the EFT operators dominate, one can not simply discard the $\langle \mathcal{M}_{\text{SM}}^2 \rangle$ term in eq. (4.5) since for some of the operators in table 1, for example, the $\mathcal{O}_{3,4,5}^6$ operators, the $\langle \mathcal{M}_{\text{SM}}^2 \rangle$ is the only part that tells how T_γ and T_{ν_α} evolve with time as we will see below. In light of this, we always keep all the three terms in eq. (4.5) during our calculation, while using the large Λ limit to cross check our results.

By plugging in \mathcal{M}_{SM} and \mathcal{M}_{EFT} in eq. (4.5), one obtains $\langle \mathcal{M}^2 \rangle_{1+2 \rightarrow 3+4}$ as a function of p_{ij} , the SM model parameters, the scale of new physics Λ , and the Wilson coefficients C_j in the last column of table 1. One can then calculate the collision term integrals through finishing the integral shown in eq. (3.11). However, due to momentum-energy conservation, redundancy exists in the calculation of collision term integrals. This redundancy can be sufficiently removed by first choosing a set of basis, which we discuss in the next subsection.

4.2 Choices of the independent bases

To start, we realize that for both the SM and the EFT contributions, the relevant processes are either $2 \rightarrow 2$ scattering or $2 \rightarrow 2$ annihilating processes. Denoting these processes generically as $1+2 \rightarrow 3+4$ with momentum p_i for the i -th particle, the invariant amplitude $\langle \mathcal{M}^2 \rangle_{1+2 \rightarrow 3+4}$, defined in eq. (4.5), can be expressed as a tower of the momentum scalar product p_{ij} defined in eq. (3.20):

$$\langle \mathcal{M}^2 \rangle_{1+2 \rightarrow 3+4} = \sum_{i, \dots, t=1}^4 \sum_{k=0}^{\infty} c_{ij \dots mn \dots st}(\{m\}, \{g\}, \{C\}, \Lambda, \{T\}, \{\mu\}) \cdot \underbrace{p_{ij} \cdots p_{mn} \cdots p_{st}}_{k = \text{number of } p_{ij}\text{'s}}, \quad (4.6)$$

⁹The collision term integrals for the $\nu_\alpha \nu_\alpha \rightarrow \gamma^* \rightarrow \nu_\alpha \nu_\alpha$ process simply vanish since the initial and the final states have exactly the same temperature, thus the number density and the energy densities of ν_α remain the same before and after the interaction.

k	Bases	Number of bases
0	1	1
1	p_{12}, p_{13}, p_{14}	3
2	$p_{12}^2, p_{12} \cdot p_{13}, p_{12} \cdot p_{14}, p_{13}^2, p_{13} \cdot p_{14}, p_{14}^2$	6
3	$p_{12}^3, p_{12}^2 \cdot p_{13}, p_{12}^2 \cdot p_{14}, p_{12} \cdot p_{13}^2, p_{12} \cdot p_{13} \cdot p_{14}, p_{12} \cdot p_{14}^2$ $p_{13}^3, p_{13}^2 \cdot p_{14}, p_{13} \cdot p_{14}^2, p_{14}^3$	10

Table 2. The bases we choose with different k 's for the calculation of collision term integrals. See the main text for more discussion.

where the coefficients $c_{ij\dots mn\dots st}$'s are generically functions of the mass set $\{m\}$ and the coupling set $\{g\}$ of the SM, the new physics scale Λ and the corresponding Wilson coefficient set $\{C\}$ in the last column of table 1, the temperatures T_{γ,ν_α} and the chemical potentials μ_{γ,ν_α} .

In this work, since we are only interested in contributions from the SM and the EFT operators up to dimension-7 as listed in table 1, it turns out that we only need to consider k 's up to $k = 3$ in eq. (4.6), which then gives, by leaving out the arguments of $c_{ij\dots mn\dots st}$'s,

$$\begin{aligned}
 \langle \mathcal{M}^2 \rangle_{1+2 \rightarrow 3+4} = & c_0 + \sum_{\substack{i,j=1 \\ i \neq j}}^4 c_{ij} \cdot p_{ij} + \sum_{\substack{i,\dots,n=1 \\ i \neq j \\ m \neq n}}^4 c_{ijmn} \cdot p_{ij} \cdot p_{mn} \\
 & + \sum_{\substack{i,\dots,t=1 \\ i \neq j \\ m \neq n \\ s \neq t}}^4 c_{ijmnst} \cdot p_{ij} \cdot p_{mn} \cdot p_{st}. \tag{4.7}
 \end{aligned}$$

Note that for $k = 1$, and similarly for the $k = 2, 3$ cases, we have included contributions from $i = j$ in the c_0 term from the on-shell conditions. On the other hand, terms in the second and the third lines of eq. (4.7) are not all independent from momentum-energy conservation, resulting in redundancy when one calculates the collision term integrals from eqs. (4.7) and (3.11). However, this redundancy can be sufficiently removed by first choosing an independent basis in terms of p_{ij} , and then rewriting $\langle \mathcal{M}^2 \rangle_{1+2 \rightarrow 3+4}$ as a linear combination of these bases. Depending on k , the independent bases we choose are presented in table 2. One can then readily express the momentum tower as linear combinations of these bases. For example,

$$\begin{aligned}
 p_{12} \cdot p_{23} \cdot p_{24} = & \frac{1}{4} \left((m_1^2 - m_2^2)^2 - (m_3^2 - m_4^2)^2 \right) p_{12} + \frac{1}{2} (m_2^2 + m_3^2 - m_1^2 - m_4^2) p_{12} \cdot p_{13} \\
 & + \frac{1}{2} (m_2^2 + m_4^2 - m_1^2 - m_3^2) p_{12} \cdot p_{14} + p_{12} \cdot p_{13} \cdot p_{14} \tag{4.8}
 \end{aligned}$$

$$\rightarrow p_{12} \cdot p_{13} \cdot p_{14} \quad \text{in the massless limit.} \tag{4.9}$$

At this stage, the collision term integral in eq. (3.11) boils down to the collision term integral with $\langle \mathcal{M}^2 \rangle_{1+2 \rightarrow 3+4}$ being replaced by the independent bases shown in table 2.

Particularly, when all the masses involved are vanishing, $\langle \mathcal{M}^2 \rangle_{1+2 \rightarrow 3+4}$ generically simplifies significantly as seen from the example above. Therefore, as also discussed at the end of section 3.2, to obtain analytical results for the collision term integrals, we assume $m_i = 0$ ($i = 1, \dots, 4$)¹⁰ and all particles obey the Maxwell-Boltzmann distribution. We then present the complete generic and analytical dictionary of the collision term integrals in section 4.4. Corrections from finite electron mass m_e , spin statistics and neutrino chemical potentials are discussed in section 4.3.

4.3 Corrections from m_e , spin statistics and chemical potentials

As already noticed in ref. [125], corrections from finite electron mass m_e and spin-statistics have to be included to reproduce N_{eff} obtained from the density matrix formalism. Furthermore, as one can see from table 1 of ref. [125], these corrections are of the same order as the finite temperature corrections discussed at the beginning of this section. Thus, to be consistent, these corrections have to be included.

In ref. [125], finite m_e corrections are obtained by finding the ratios of the collision term integrals in eq. (3.11) by switching on and off m_e . Similarly, corrections from spin statistics are computed by finding the ratios of the collision term integrals with Fermi-Dirac/Bose-Einstein and Maxwell-Boltzmann distributions respectively. For a detailed discussion, see refs. [125, 126]. Though the methods used for the collision term integrals are different, we reproduce the numbers in table 6 of ref. [125] and/or table III of ref. [126]. These corrections are then included in the Boltzmann equations and used to solve N_{eff} . The results are presented and discussed in more detail in section 5.

We also comment on that neutrino chemical potentials are highly suppressed due to the rapid $\bar{\nu}\nu \leftrightarrow e^+e^- \leftrightarrow \gamma\gamma$ conversion and that the electron chemical potential is negligibly small compared to the plasma temperature in the early Universe. In our setup, in order to be generic, we keep neutrino chemical potentials throughout our analytical calculations, but stress that they would have no visible impact on the current/planned precision measurement of N_{eff} . For our numerical calculations, we choose $\mu_\nu = \mu_{\bar{\nu}}$ and $|\mu_\nu/T_\gamma| = 10^{-4}$ with $T_\gamma = T_\nu = 10 \text{ MeV}$ as our initial conditions, and verify that this setup is numerically equivalent to vanishing neutrino chemical potentials as expected.

4.4 A complete generic and analytical dictionary of the collision term integrals

In last subsection, we list in table 2 the independent bases by which the invariant amplitudes $\langle \mathcal{M}^2 \rangle_{1+2 \rightarrow 3+4}$ can be expressed, and conclude that the redundancy of collision term integrals from momentum-energy conservation can be removed by working with these bases directly. In this subsection, we provide the complete analytical dictionary of the collision term integrals for particle “1” and up to $k = 3$, with k the number of p_{ij} ’s in the invariant amplitude. We note that a subset of this complete dictionary was presented in the appendices of refs. [124, 126], which agrees with our results presented in this subsection as long as one specifies T_i and μ_i accordingly.

¹⁰Since the electron mass m_e is the only one matters here, this assumption basically means that, when calculating the collision term integrals in eq. (3.11), we take the untra-relativistic limit for electrons in the early Universe.

For the collision term integrals, we follow the procedure briefly summarized in section 3.2 and stick to our notation in eq. (3.11), where $j = 0$ represents the collision term integral for the number density and $j = 1$ that for the energy density. The dependence on p_{ij} of $\langle \mathcal{M}^2 \rangle_{1+2 \rightarrow 3+4}$ is reflected by the argument of $C^{(j)}$.¹¹ For example, $C^{(0)}(p_{12})$ means the collision term integral for the number density with $\langle \mathcal{M}^2 \rangle_{1+2 \rightarrow 3+4} = p_{12}$ ¹² in eq. (3.11).

4.4.1 $\langle \mathcal{M}^2 \rangle_{1+2 \rightarrow 3+4} = 1$

$$C^{(j)}(1) = \begin{cases} \frac{1}{128\pi^5} \left[-e^{\frac{\mu_1}{T_1} + \frac{\mu_2}{T_2}} T_1^2 T_2^2 + e^{\frac{\mu_3}{T_3} + \frac{\mu_4}{T_4}} T_3^2 T_4^2 \right], & j = 0 \\ \frac{1}{128\pi^5} \left[-2e^{\frac{\mu_1}{T_1} + \frac{\mu_2}{T_2}} T_1^3 T_2^2 + e^{\frac{\mu_3}{T_3} + \frac{\mu_4}{T_4}} T_3^2 T_4^2 (T_3 + T_4) \right], & j = 1 \end{cases}, \quad (4.10)$$

From eq. (4.10), one notes that in the $j = 0$ case, the collision term integral, corresponding to the number density, vanishes when $T_1 = T_3$ and $T_2 = T_4$. This is expected since it actually stands for a scattering process where the number density for each species remains the same before and after the interaction. This conclusion holds generically and is independent of the form of $\langle \mathcal{M}^2 \rangle_{1+2 \rightarrow 3+4}$, as one can also see clearly from the results below. On the other hand, if $T_1 = T_2 = T_3 = T_4$ and $\mu_1 = \mu_2 = \mu_3 = \mu_4$, then all the $C^{(j)}$'s vanish, which is also as expected since particle self interactions do not modify the number and the energy densities as long as thermal equilibrium is maintained. This observation also acts as a cross-check of our analytical results presented in these subsections.

4.4.2 $\langle \mathcal{M}^2 \rangle_{1+2 \rightarrow 3+4} = p_{ij}$

$$C^{(j)}(p_{12}) = \begin{cases} \frac{1}{32\pi^5} \left[-e^{\frac{\mu_1}{T_1} + \frac{\mu_2}{T_2}} T_1^3 T_2^3 + e^{\frac{\mu_3}{T_3} + \frac{\mu_4}{T_4}} T_3^3 T_4^3 \right], & j = 0 \\ \frac{1}{64\pi^5} \left[-6e^{\frac{\mu_1}{T_1} + \frac{\mu_2}{T_2}} T_1^4 T_2^3 + 3e^{\frac{\mu_3}{T_3} + \frac{\mu_4}{T_4}} T_3^3 T_4^3 (T_3 + T_4) \right], & j = 1 \end{cases}, \quad (4.11)$$

$$C^{(j)}(p_{13}) = \begin{cases} \frac{1}{64\pi^5} \left[-e^{\frac{\mu_1}{T_1} + \frac{\mu_2}{T_2}} T_1^3 T_2^3 + e^{\frac{\mu_3}{T_3} + \frac{\mu_4}{T_4}} T_3^3 T_4^3 \right], & j = 0 \\ \frac{1}{64\pi^5} \left[-3e^{\frac{\mu_1}{T_1} + \frac{\mu_2}{T_2}} T_1^4 T_2^3 + e^{\frac{\mu_3}{T_3} + \frac{\mu_4}{T_4}} T_3^3 T_4^3 (T_3 + 2T_4) \right], & j = 1 \end{cases}, \quad (4.12)$$

$$C^{(j)}(p_{14}) = \begin{cases} \frac{1}{64\pi^5} \left[-e^{\frac{\mu_1}{T_1} + \frac{\mu_2}{T_2}} T_1^3 T_2^3 + e^{\frac{\mu_3}{T_3} + \frac{\mu_4}{T_4}} T_3^3 T_4^3 \right], & j = 0 \\ \frac{1}{64\pi^5} \left[-3e^{\frac{\mu_1}{T_1} + \frac{\mu_2}{T_2}} T_1^4 T_2^3 + e^{\frac{\mu_3}{T_3} + \frac{\mu_4}{T_4}} T_3^3 T_4^3 (2T_3 + T_4) \right], & j = 1 \end{cases}, \quad (4.13)$$

¹¹We stress that the argument of $C^{(j)}$ here is only used to reflect the dependence on p_{ij} of $\langle \mathcal{M}^2 \rangle_{1+2 \rightarrow 3+4}$, and this argument does not mean that $C^{(j)}$ depends on p_{ij} . Instead, $C^{(j)}$ only depends on the model parameters, the new physics scale, the Wilson coefficients, the temperatures T_{γ, ν_α} and the chemical potentials μ_{ν_α} .

¹²We leave out any overall factors in $\langle \mathcal{M}^2 \rangle_{1+2 \rightarrow 3+4}$ that are independent of p_{ij} here and in the following.

4.4.3 $\langle \mathcal{M}^2 \rangle_{1+2 \rightarrow 3+4} = \mathbf{p}_{ij} \cdot \mathbf{p}_{mn}$

$$C^{(j)}(p_{12}^2) = \begin{cases} \frac{3}{8\pi^5} \left[-e^{\frac{\mu_1}{T_1} + \frac{\mu_2}{T_2}} T_1^4 T_2^4 + e^{\frac{\mu_3}{T_3} + \frac{\mu_4}{T_4}} T_3^4 T_4^4 \right], & j = 0 \\ \frac{1}{4\pi^5} \left[-6e^{\frac{\mu_1}{T_1} + \frac{\mu_2}{T_2}} T_1^5 T_2^4 + 3e^{\frac{\mu_3}{T_3} + \frac{\mu_4}{T_4}} T_3^4 T_4^4 (T_3 + T_4) \right], & j = 1 \end{cases}, \quad (4.14)$$

$$C^{(j)}(p_{12} \cdot p_{13}) = \begin{cases} \frac{3}{16\pi^5} \left[-e^{\frac{\mu_1}{T_1} + \frac{\mu_2}{T_2}} T_1^4 T_2^4 + e^{\frac{\mu_3}{T_3} + \frac{\mu_4}{T_4}} T_3^4 T_4^4 \right], & j = 0 \\ \frac{1}{4\pi^5} \left[-3e^{\frac{\mu_1}{T_1} + \frac{\mu_2}{T_2}} T_1^5 T_2^4 + e^{\frac{\mu_3}{T_3} + \frac{\mu_4}{T_4}} T_3^4 T_4^4 (T_3 + 2T_4) \right], & j = 1 \end{cases}, \quad (4.15)$$

$$C^{(j)}(p_{12} \cdot p_{14}) = \begin{cases} \frac{3}{16\pi^5} \left[-e^{\frac{\mu_1}{T_1} + \frac{\mu_2}{T_2}} T_1^4 T_2^4 + e^{\frac{\mu_3}{T_3} + \frac{\mu_4}{T_4}} T_3^4 T_4^4 \right], & j = 0 \\ \frac{1}{4\pi^5} \left[-3e^{\frac{\mu_1}{T_1} + \frac{\mu_2}{T_2}} T_1^5 T_2^4 + e^{\frac{\mu_3}{T_3} + \frac{\mu_4}{T_4}} T_3^4 T_4^4 (2T_3 + T_4) \right], & j = 1 \end{cases}, \quad (4.16)$$

$$C^{(j)}(p_{13}^2) = \begin{cases} \frac{1}{8\pi^5} \left[-e^{\frac{\mu_1}{T_1} + \frac{\mu_2}{T_2}} T_1^4 T_2^4 + e^{\frac{\mu_3}{T_3} + \frac{\mu_4}{T_4}} T_3^4 T_4^4 \right], & j = 0 \\ \frac{1}{8\pi^5} \left[-4e^{\frac{\mu_1}{T_1} + \frac{\mu_2}{T_2}} T_1^5 T_2^4 + e^{\frac{\mu_3}{T_3} + \frac{\mu_4}{T_4}} T_3^4 T_4^4 (T_3 + 3T_4) \right], & j = 1 \end{cases}, \quad (4.17)$$

$$C^{(j)}(p_{13} \cdot p_{14}) = \begin{cases} \frac{1}{16\pi^5} \left[-e^{\frac{\mu_1}{T_1} + \frac{\mu_2}{T_2}} T_1^4 T_2^4 + e^{\frac{\mu_3}{T_3} + \frac{\mu_4}{T_4}} T_3^4 T_4^4 \right], & j = 0 \\ \frac{1}{8\pi^5} \left[-2e^{\frac{\mu_1}{T_1} + \frac{\mu_2}{T_2}} T_1^5 T_2^4 + e^{\frac{\mu_3}{T_3} + \frac{\mu_4}{T_4}} T_3^4 T_4^4 (T_3 + T_4) \right], & j = 1 \end{cases}, \quad (4.18)$$

$$C^{(j)}(p_{14}^2) = \begin{cases} \frac{1}{8\pi^5} \left[-e^{\frac{\mu_1}{T_1} + \frac{\mu_2}{T_2}} T_1^4 T_2^4 + e^{\frac{\mu_3}{T_3} + \frac{\mu_4}{T_4}} T_3^4 T_4^4 \right], & j = 0 \\ \frac{1}{8\pi^5} \left[-4e^{\frac{\mu_1}{T_1} + \frac{\mu_2}{T_2}} T_1^5 T_2^4 + e^{\frac{\mu_3}{T_3} + \frac{\mu_4}{T_4}} T_3^4 T_4^4 (3T_3 + T_4) \right], & j = 1 \end{cases}, \quad (4.19)$$

4.4.4 $\langle \mathcal{M}^2 \rangle_{1+2 \rightarrow 3+4} = \mathbf{p}_{ij} \cdot \mathbf{p}_{mn} \cdot \mathbf{p}_{st}$

$$C^{(j)}(p_{12}^3) = \begin{cases} -\frac{9}{\pi^5} \left[e^{\frac{\mu_1}{T_1} + \frac{\mu_2}{T_2}} T_1^5 T_2^5 - e^{\frac{\mu_3}{T_3} + \frac{\mu_4}{T_4}} T_3^5 T_4^5 \right], & j = 0 \\ -\frac{45}{2\pi^5} \left[2e^{\frac{\mu_1}{T_1} + \frac{\mu_2}{T_2}} T_1^6 T_2^5 - e^{\frac{\mu_3}{T_3} + \frac{\mu_4}{T_4}} T_3^5 T_4^5 (T_3 + T_4) \right], & j = 1 \end{cases}, \quad (4.20)$$

$$C^{(j)}(p_{12}^2 \cdot p_{13}) = \begin{cases} -\frac{9}{2\pi^5} \left[e^{\frac{\mu_1}{T_1} + \frac{\mu_2}{T_2}} T_1^5 T_2^5 - e^{\frac{\mu_3}{T_3} + \frac{\mu_4}{T_4}} T_3^5 T_4^5 \right], & j = 0 \\ -\frac{15}{2\pi^5} \left[3e^{\frac{\mu_1}{T_1} + \frac{\mu_2}{T_2}} T_1^6 T_2^5 - e^{\frac{\mu_3}{T_3} + \frac{\mu_4}{T_4}} T_3^5 T_4^5 (T_3 + 2T_4) \right], & j = 1 \end{cases}, \quad (4.21)$$

$$C^{(j)}(p_{12}^2 \cdot p_{14}) = \begin{cases} -\frac{9}{2\pi^5} \left[e^{\frac{\mu_1}{T_1} + \frac{\mu_2}{T_2}} T_1^5 T_2^5 - e^{\frac{\mu_3}{T_3} + \frac{\mu_4}{T_4}} T_3^5 T_4^5 \right], & j = 0 \\ -\frac{15}{2\pi^5} \left[3e^{\frac{\mu_1}{T_1} + \frac{\mu_2}{T_2}} T_1^6 T_2^5 - e^{\frac{\mu_3}{T_3} + \frac{\mu_4}{T_4}} T_3^5 T_4^5 (2T_3 + T_4) \right], & j = 1 \end{cases}, \quad (4.22)$$

$$C^{(j)}(p_{12} \cdot p_{13}^2) = \begin{cases} -\frac{3}{\pi^5} \left[e^{\frac{\mu_1}{T_1} + \frac{\mu_2}{T_2}} T_1^5 T_2^5 - e^{\frac{\mu_3}{T_3} + \frac{\mu_4}{T_4}} T_3^5 T_4^5 \right], & j = 0 \\ -\frac{15}{4\pi^5} \left[4e^{\frac{\mu_1}{T_1} + \frac{\mu_2}{T_2}} T_1^6 T_2^5 - e^{\frac{\mu_3}{T_3} + \frac{\mu_4}{T_4}} T_3^5 T_4^5 (T_3 + 3T_4) \right], & j = 1 \end{cases}, \quad (4.23)$$

$$C^{(j)}(p_{12} \cdot p_{13} \cdot p_{14}) = \begin{cases} \frac{3}{2\pi^5} \left[-e^{\frac{\mu_1}{T_1} + \frac{\mu_2}{T_2}} T_1^5 T_2^5 + e^{\frac{\mu_3}{T_3} + \frac{\mu_4}{T_4}} T_3^5 T_4^5 \right], & j = 0 \\ \frac{15}{4\pi^5} \left[-2e^{\frac{\mu_1}{T_1} + \frac{\mu_2}{T_2}} T_1^6 T_2^5 + e^{\frac{\mu_3}{T_3} + \frac{\mu_4}{T_4}} T_3^5 T_4^5 (T_3 + T_4) \right], & j = 1 \end{cases}, \quad (4.24)$$

$$C^{(j)}(p_{12} \cdot p_{14}^2) = \begin{cases} -\frac{3}{\pi^5} \left[e^{\frac{\mu_1}{T_1} + \frac{\mu_2}{T_2}} T_1^5 T_2^5 - e^{\frac{\mu_3}{T_3} + \frac{\mu_4}{T_4}} T_3^5 T_4^5 \right], & j = 0 \\ -\frac{15}{4\pi^5} \left[4e^{\frac{\mu_1}{T_1} + \frac{\mu_2}{T_2}} T_1^6 T_2^5 - e^{\frac{\mu_3}{T_3} + \frac{\mu_4}{T_4}} T_3^5 T_4^5 (3T_3 + T_4) \right], & j = 1 \end{cases}, \quad (4.25)$$

$$C^{(j)}(p_{13}^3) = \begin{cases} \frac{9}{4\pi^5} \left[-e^{\frac{\mu_1}{T_1} + \frac{\mu_2}{T_2}} T_1^5 T_2^5 + e^{\frac{\mu_3}{T_3} + \frac{\mu_4}{T_4}} T_3^5 T_4^5 \right], & j = 0 \\ \frac{9}{4\pi^5} \left[-5e^{\frac{\mu_1}{T_1} + \frac{\mu_2}{T_2}} T_1^6 T_2^5 + e^{\frac{\mu_3}{T_3} + \frac{\mu_4}{T_4}} T_3^5 T_4^5 (T_3 + 4T_4) \right], & j = 1 \end{cases}, \quad (4.26)$$

$$C^{(j)}(p_{13}^2 \cdot p_{14}) = \begin{cases} -\frac{3}{4\pi^5} \left[e^{\frac{\mu_1}{T_1} + \frac{\mu_2}{T_2}} T_1^5 T_2^5 - e^{\frac{\mu_3}{T_3} + \frac{\mu_4}{T_4}} T_3^5 T_4^5 \right], & j = 0 \\ -\frac{3}{4\pi^5} \left[5e^{\frac{\mu_1}{T_1} + \frac{\mu_2}{T_2}} T_1^6 T_2^5 - e^{\frac{\mu_3}{T_3} + \frac{\mu_4}{T_4}} T_3^5 T_4^5 (2T_3 + 3T_4) \right], & j = 1 \end{cases}, \quad (4.27)$$

$$C^{(j)}(p_{13} \cdot p_{14}^2) = \begin{cases} -\frac{3}{4\pi^5} \left[e^{\frac{\mu_1}{T_1} + \frac{\mu_2}{T_2}} T_1^5 T_2^5 - e^{\frac{\mu_3}{T_3} + \frac{\mu_4}{T_4}} T_3^5 T_4^5 \right], & j = 0 \\ -\frac{3}{4\pi^5} \left[5e^{\frac{\mu_1}{T_1} + \frac{\mu_2}{T_2}} T_1^6 T_2^5 - e^{\frac{\mu_3}{T_3} + \frac{\mu_4}{T_4}} T_3^5 T_4^5 (3T_3 + 2T_4) \right], & j = 1 \end{cases}, \quad (4.28)$$

$$C^{(j)}(p_{14}^3) = \begin{cases} -\frac{9}{4\pi^5} \left[e^{\frac{\mu_1}{T_1} + \frac{\mu_2}{T_2}} T_1^5 T_2^5 - e^{\frac{\mu_3}{T_3} + \frac{\mu_4}{T_4}} T_3^5 T_4^5 \right], & j = 0 \\ -\frac{9}{4\pi^5} \left[5e^{\frac{\mu_1}{T_1} + \frac{\mu_2}{T_2}} T_1^6 T_2^5 - e^{\frac{\mu_3}{T_3} + \frac{\mu_4}{T_4}} T_3^5 T_4^5 (4T_3 + T_4) \right], & j = 1 \end{cases}, \quad (4.29)$$

With this complete dictionary, one can readily write down the Boltzmann equations for T_γ and T_ν as long as $\langle \mathcal{M}^2 \rangle_{1+2 \rightarrow 3+4}$ in eqs. (3.8)–(3.9) is known. For example, besides SM contributions, only the $\mathcal{O}_{3,4,5}^{(6)}$ operators listed in table 1 introduce new neutrino self-interactions and thus modify the number and the energy densities of neutrinos of different

flavors. For the $\nu_\alpha\nu_\beta \rightarrow \nu_\alpha\nu_\beta$ ($\alpha \neq \beta$) process, we find

$$\begin{aligned} \langle \mathcal{M}^2 \rangle_{\nu_\alpha\nu_\beta \rightarrow \nu_\alpha\nu_\beta}^{\text{SM}+\mathcal{O}_{3,4,5}^{(6)}} = & \left[32G_F^2 \cdot p_{12}^2 + \frac{32\sqrt{2}G_F C_4^{(6)}}{\Lambda^2} \cdot p_{12}^2 + \frac{16}{\Lambda^4} \left((C_4^{(6)})^2 - 2(C_3^{(6)} - 4C_5^{(6)})C_5^{(6)} \right) \cdot p_{12}^2 \right. \\ & \left. + \frac{4}{\Lambda^4} \left((C_3^{(6)})^2 - 16(C_5^{(6)})^2 \right) \cdot p_{13}^2 + \frac{32C_5^{(6)}}{\Lambda^4} \left(C_3^{(6)} + 4C_5^{(6)} \right) \cdot p_{14}^2 \right], \end{aligned} \quad (4.30)$$

where G_F is the Fermi constant and Λ is the scale of the potential new physics. The first term in the square bracket is the pure SM contributions, the second term is the interference term between the SM and the $\mathcal{O}_4^{(6)}$ operator, and the remaining terms are the pure contributions from the $\mathcal{O}_{3,4,5}^{(6)}$ operators. One can then immediately write down the collision term integrals for the $\nu_\alpha\nu_\beta \rightarrow \nu_\alpha\nu_\beta$ process as

$$\begin{aligned} C_{\nu_\alpha\nu_\beta \rightarrow \nu_\alpha\nu_\beta}^{(j)} = & \left[32G_F^2 \cdot C^{(j)}(p_{12}^2) + \frac{32\sqrt{2}G_F C_4^{(6)}}{\Lambda^2} \cdot C^{(j)}(p_{12}^2) \right. \\ & + \frac{16}{\Lambda^4} \left((C_4^{(6)})^2 - 2(C_3^{(6)} - 4C_5^{(6)})C_5^{(6)} \right) \cdot C^{(j)}(p_{12}^2) \\ & + \frac{4}{\Lambda^4} \left((C_3^{(6)})^2 - 16(C_5^{(6)})^2 \right) \cdot C^{(j)}(p_{13}^2) \\ & \left. + \frac{32C_5^{(6)}}{\Lambda^4} \left(C_3^{(6)} + 4C_5^{(6)} \right) \cdot C^{(j)}(p_{14}^2) \right], \end{aligned} \quad (4.31)$$

where $C^{(j)}(p_{12}^2)$, $C^{(j)}(p_{13}^2)$ and $C^{(j)}(p_{14}^2)$ are given in eqs. (4.14), (4.17) and (4.19) respectively, and $j = 0(1)$ is for the number (energy) density of ν_α . Though not shown explicitly, $C^{(j)}(p_{12}^2)$, $C^{(j)}(p_{13}^2)$ and $C^{(j)}(p_{14}^2)$ depend on the temperatures and the chemical potentials of $\nu_{\alpha,\beta}$. Specifically, one has $T_{1,3} = T_{\nu_\alpha}$, $T_{2,4} = T_{\nu_\beta}$, $\mu_{1,3} = \mu_{\nu_\alpha}$, $\mu_{2,4} = \mu_{\nu_\beta}$ for $\alpha, \beta = e, \mu, \tau$ and $\alpha \neq \beta$.

The complete results of $\langle \mathcal{M}^2 \rangle$ from SM and the EFT operators listed in table 1 are given in the supplementary material as a `Mathematica` notebook file for all relevant processes, together with all the replacement rules to rewrite $\langle \mathcal{M}^2 \rangle$ in terms of the bases listed in table 2.¹³ We point out that when all the Wilson coefficients vanish therein, we reproduce the SM results as presented in, for example, ref. [173]. Using the complete dictionary summarized in this section and building our code upon `nudec_BSM` from ref. [125], we study corrections to N_{eff} from the NSI operators in table 1, and discuss the results in section 5.

5 Constraints on EFT operators from N_{eff}

With the complete dictionary presented in section 4, one can readily solve the Boltzmann equations for T_γ and T_{ν_α} , and thus obtain corrections to N_{eff} . In what follows, we define these corrections as

$$\Delta N_{\text{eff}} = N_{\text{eff}}^{\text{SM+EFT}} - N_{\text{eff}}^{\text{SM}}, \quad (5.1)$$

¹³The replacement rules are obtained with the help of `Package-X` [172].

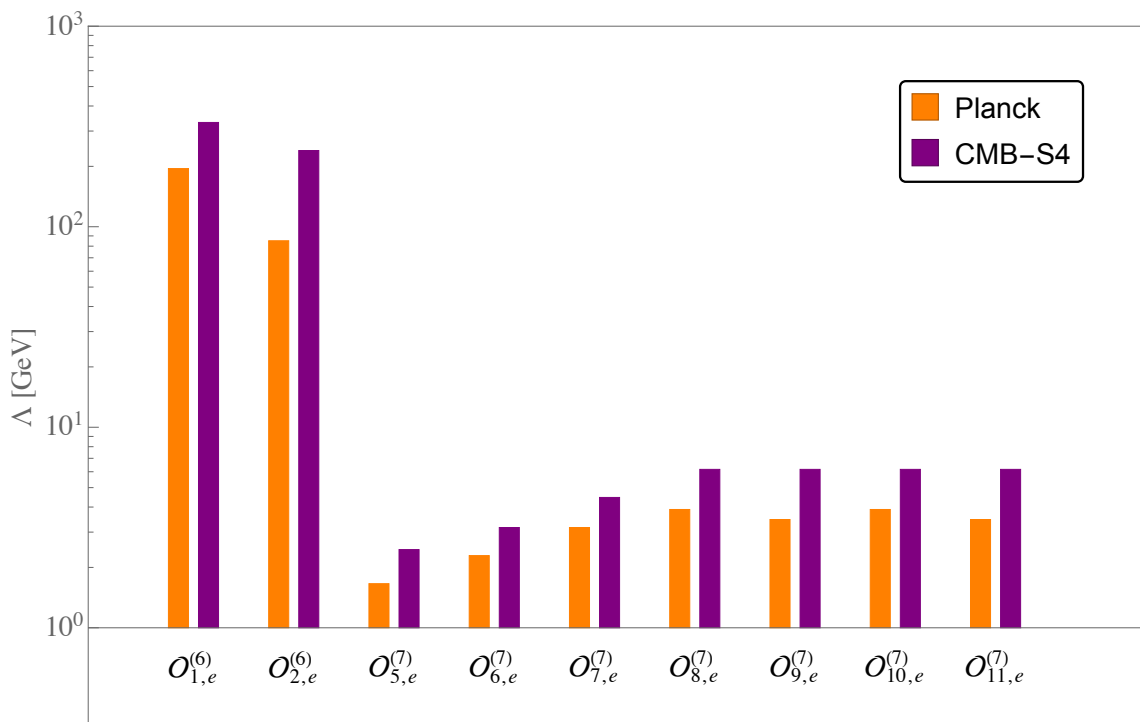


Figure 1. Constraints on the characteristic scale Λ of new physics from $\Delta N_{\text{eff}} = N_{\text{eff}}^{\text{SM+EFT}} - N_{\text{eff}}^{\text{SM}}$, where $N_{\text{eff}}^{\text{SM}} = 3.044$ [123, 132] is the SM prediction of N_{eff} , and $N_{\text{eff}}^{\text{SM+EFT}}$ is that from SM and new physics. Note that the plot is obtained by fixing all Wilson coefficients at unity and considering only one non-vanishing operator only at a time. See the main text for more discussion.

where $N_{\text{eff}}^{\text{SM+EFT}}$ is the theoretical prediction of N_{eff} with the inclusion of the NC NSI operators, and $N_{\text{eff}}^{\text{SM}} = 3.044$ [123, 132] that from the pure SM. For Planck, we use the current result $N_{\text{eff}} = 2.99_{-0.33}^{+0.34}$ [114] at the 95% CL to obtain the constraints, and $\Delta N_{\text{eff}} < 0.06$ at 95% CL for CMB-S4 [117, 143, 144, 146].

Our code is built upon `nudec_BSM` from ref. [125], and is then used to solve eqs. (3.8)–(3.9) numerically by `Mathematica`. During our numerical solutions, we keep terms proportional to m_e in $\langle \mathcal{M}^2 \rangle$ and assume $T_{\nu_\mu} = T_{\nu_\tau} \neq T_{\nu_e}$ and $\mu_{\nu_\mu} = \mu_{\nu_\tau} \neq \mu_{\nu_e}$. In the very large Λ limit, we reproduce the results in table 1 of ref. [125] for both $T_{\nu_e} = T_{\nu_{\mu,\tau}}$ and $T_{\nu_e} \neq T_{\nu_{\mu,\tau}}$. We then show our results for varying Wilson coefficients or the new physics scale Λ in the following subsections.

5.1 Constraints on Λ with fixed Wilson coefficients

Following the notations clarified in table 1 and fixing the Wilson coefficients at unity, we present our results in figure 1. The constraints shown in figure 1 are obtained by assuming only one non-vanishing NSI operator at a time, and the results are presented from considering the latest results from Planck [114] in orange and the proposed precision goal of CMB-S4 [117, 143, 144, 146] in purple. Several points from this plot merit emphasizing:

Operators	Lower bound on Λ [GeV]	
	Planck	CMB-S4
$\mathcal{O}_{1,e}^{(6)}$	194.98	331.13
$\mathcal{O}_{2,e}^{(6)}$	85.11	239.88, except (94.84, 102.33)
$\mathcal{O}_{5,e}^{(7)}$	1.66	2.45, except (1.91, 2.45)
$\mathcal{O}_{6,e}^{(7)}$	2.29	3.16
$\mathcal{O}_{7,e}^{(7)}$	3.16	4.47
$\mathcal{O}_{8,e}^{(7)}$	3.89	6.17
$\mathcal{O}_{9,e}^{(7)}$	3.47	6.17
$\mathcal{O}_{10,e}^{(7)}$	3.89	6.17
$\mathcal{O}_{11,e}^{(7)}$	3.47	6.17

Table 3. Constraints on EFT operators from current Planck data and future CMB-S4 proposal. All lower bounds are obtained by assuming one non-vanishing EFT operator at a time and fixing the Wilson coefficients at unity. Note that for $\mathcal{O}_{2,e}^{(6)}$ and $\mathcal{O}_{5,f}^{(7)}$, there are exception intervals for CMB-S4 as a result of destructive interference or a negative shift in N_{eff} from the EFT operators. See the main text for more discussion.

- Constraints on dimension-6 EFT operators are generically stronger than those on the dimension-7 ones. The reason is that dimension-7 operators are more suppressed by one more power of Λ . Moreover, among the dimension-6 operators, currently, the Planck data leads to the most stringent constraint on the $\mathcal{O}_{1,e}^{(6)}$ operator, whose lower bound is presently constrained to be about 195 GeV. In the future, CMB-S4 would improve this lower bound to about 240 GeV, as one can see from the first purple histogram in figure 1. Quantitatively, we summarize the lower bounds on Λ 's for all the operators shown in figure 1 in table 3.
- As one can see from table 3, for the $\mathcal{O}_{2,e}^{(6)}$ and $\mathcal{O}_{5,f}^{(7)}$ operators, there exist intervals that can not be covered by future CMB-S4 if one considers only one operator at a time. However, if one considers multiple operators, these two exception intervals would be ruled out by future CMB-S4 result. For this reason, figure 1 is plotted by using the lower bounds 239.88 GeV and 2.45 GeV for $\mathcal{O}_{2,e}^{(6)}$ and $\mathcal{O}_{5,f}^{(7)}$ respectively. On the other hand, the exception interval for $\mathcal{O}_{2,e}^{(6)}$ results from the destructive interference between the SM and the NSI operators, while that for $\mathcal{O}_{5,f}^{(7)}$ results from a negative shift to N_{eff} when Λ is small. We show this point in the second row of figure 2.
- Constraints on dimension-6 operators $\mathcal{O}_{3,4,5}^{(6)}$ are missing in figure 1. The reason can be understood as follows: (1) When $\Lambda \gtrsim \Lambda_W$ or $\Lambda \gg \Lambda_W$, SM contributions dominate and the resulting N_{eff} always agrees with the SM prediction — The deviation of N_{eff} from the SM prediction is always within the uncertainties of both Planck and CMB-S4; (2) For $\Lambda \ll \Lambda_W$, one might naïvely think the $\langle \mathcal{M}_{\text{SM}}^2 \rangle$ term in eq. (4.5) can be safely discarded and very large N_{eff} would be predicted from $\mathcal{O}_{3,4,5}^{(6)}$. However, as we

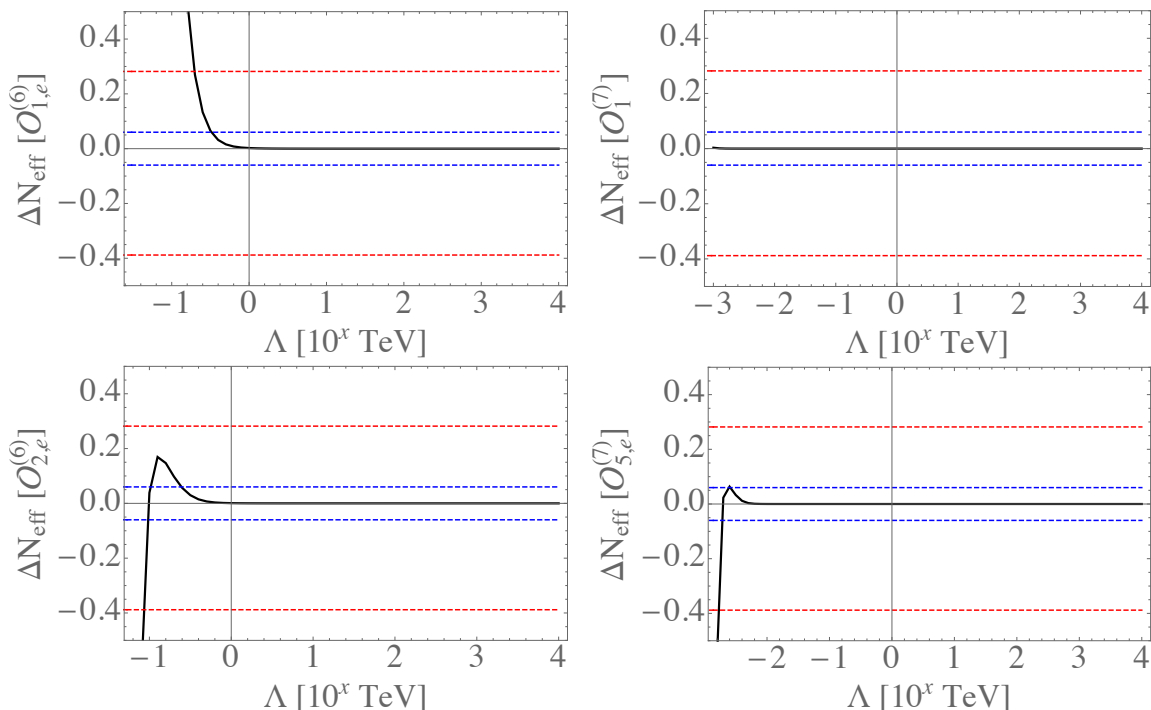


Figure 2. Corrections to N_{eff} from varying Λ . Upper left: ΔN_{eff} with the inclusion of $\mathcal{O}_{1,e}^{(6)}$ only. Very similar plots are obtained for other operators except for $\mathcal{O}_{(2,e),3,4,5}^{(6)}$, $\mathcal{O}_{1,2,(5,e)}^{(7)}$, thus we only show $\mathcal{O}_{1,e}^{(6)}$ for illustration. Upper right: ΔN_{eff} from $\mathcal{O}_1^{(7)}$ only. Very similar plot is obtained for $\mathcal{O}_2^{(7)}$. Lower left: ΔN_{eff} from $\mathcal{O}_{2,e}^{(6)}$ only. Lower right: ΔN_{eff} from $\mathcal{O}_{5,e}^{(7)}$ only. In all these subfigures, the black curve stands for corrections to N_{eff} from the related NSI operator, the horizontal red dashed line is the constraint on ΔN_{eff} from Planck, and the horizontal red dashed line is that from CMB-S4.

already point out right below eq. (4.5), the SM part can not be ignored since in this case, it is the only part that governs the evolution of T_γ . Furthermore, when $\Lambda \ll \Lambda_W$, neutrino self interactions are rapid enough to eliminate any difference between T_{ν_e} and $T_{\nu_{\mu,\tau}}$, and neutrinos of all flavors have exactly the same temperature.¹⁴ This in turn results in vanishing corrections to the collision term integrals for $\mathcal{O}_{3,4,5}^{(6)}$ as discussed right after eq. (4.10). Thus, when Λ is very small, corrections from $\mathcal{O}_{3,4,5}^{(6)}$ to N_{eff} vanish and the SM prediction is restored.

- While it is a very good approximation to neglect the temperature and the chemical differences among neutrinos when calculating N_{eff} within the SM framework, see table 1 of ref. [125] for example, this approximation does not stay valid any more in the case where new physics introduces only neutrino self interactions as the $\mathcal{O}_{3,4,5}^{(6)}$ operators.

¹⁴With our choice of the Wilson coefficients and the small Λ , neutrino self-interacting rates are always larger than the Hubble rate such that the three flavor neutrinos always stay in thermal equilibrium. However, neutrino decoupling is not affected since photon-electron-positron sector is governed by weak interactions. We emphasize that the equal temperature of neutrinos is the direct result of neutrino self-interactions introduced by $\mathcal{O}_{3,4,5}^{(6)}$, the moderate Wilson coefficients, and the small Λ .

In this scenario, if one takes the equal neutrino temperature and the equal chemical potential approximation for all the three-flavor neutrinos, then the collision term integrals simply vanish such that the effects of this new physics can never be observed.

- Constraints on $\mathcal{O}_1^{(7)}$ and $\mathcal{O}_2^{(7)}$ are also missing in figure 1, due to the suppression factors $\alpha/(12\pi)$ and $\alpha/(8\pi)$, respectively: at the amplitude level, both these two factors lead to suppression of $\mathcal{O}(10^{-4})$, thus the invariant amplitude $\langle \mathcal{M}^2 \rangle$ is suppressed by a factor of $\mathcal{O}(10^{-8})$. Note also that there is no interference between the SM and $\mathcal{O}_{1,2}^{(7)}$. The upper right panel of figure 2 shows the prediction of N_{eff} with the inclusion of $\mathcal{O}_1^{(7)}$, and similar result is obtained for $\mathcal{O}_2^{(7)}$.
- Though we do not consider the magnetic dipole operator $\mathcal{O}_1^{(5)}$ in this work, and the $\mathcal{O}_{1,2}^{(7)}$ operators are not constrained by N_{eff} as discussed above, lower bounds on Λ for these operators do exist from other experiments. For $\mathcal{O}_1^{(5)}$, it was concluded in ref. [38] that the most stringent lower bound on Λ was 2.7×10^6 GeV from the magnetic moment of ν_e using Borexino Phase-II solar neutrino data [171]. On the other hand, translating this constraint on the magnetic moment of ν_e from $\mathcal{O}_{1,2}^{(7)}$, they found $\Lambda > 328$ GeV and $\Lambda > 1081$ GeV for $\mathcal{O}_1^{(7)}$ and $\mathcal{O}_2^{(7)}$ respectively. Furthermore, $\mathcal{O}_{1,e}^{(6)}$ was also constrained to have a lower bound of 1005 GeV from a global fitting of neutrino oscillating data [38, 106]. As one can see from table 3, the constraint on $\mathcal{O}_{1,e}^{(6)}$ from the global fitting is stronger than that from N_{eff} . However, all the other operators in figure 1 are not constrained in ref. [38], making our work complementary to theirs as well as that in ref. [65].

We emphasize that conclusions above are obtained by fixing the Wilson coefficients at one and considering only one non-vanishing NSI operator at a time. In ref. [65], we find that if multiple operators exist at the same scale, then the correlation among them may change the constraints by orders of magnitude. However, due to the computation challenge, this correlation effect is in general ignored except for some UV models where the number of operators at certain dimension is limited. In this work, we find when $\Lambda \sim \Lambda_W$ or smaller where NSI contributions to $\langle \mathcal{M}^2 \rangle$ are comparable to or dominate over those from the SM, numerical computation of the Boltzmann equations is extremely slow or even impossible even with high-performance clusters. For this reason, the correlation mentioned above will not be discussed.

5.2 Constraints on Wilson coefficients with fixed Λ

Alternatively, we present the constraints for the Wilson coefficients with $\Lambda = 1$ TeV and 100 GeV in this subsection, and the results are shown in the first and the second rows of figure 3, respectively. Constraints are shown for $\mathcal{O}_{1,e}^{(6)}$ and $\mathcal{O}_{2,e}^{(6)}$ only, and all the other Wilson coefficients stay unconstrained for the range we consider in figure 3. Quantitatively, we find, assuming the same Wilson coefficients for neutrinos of different flavors,

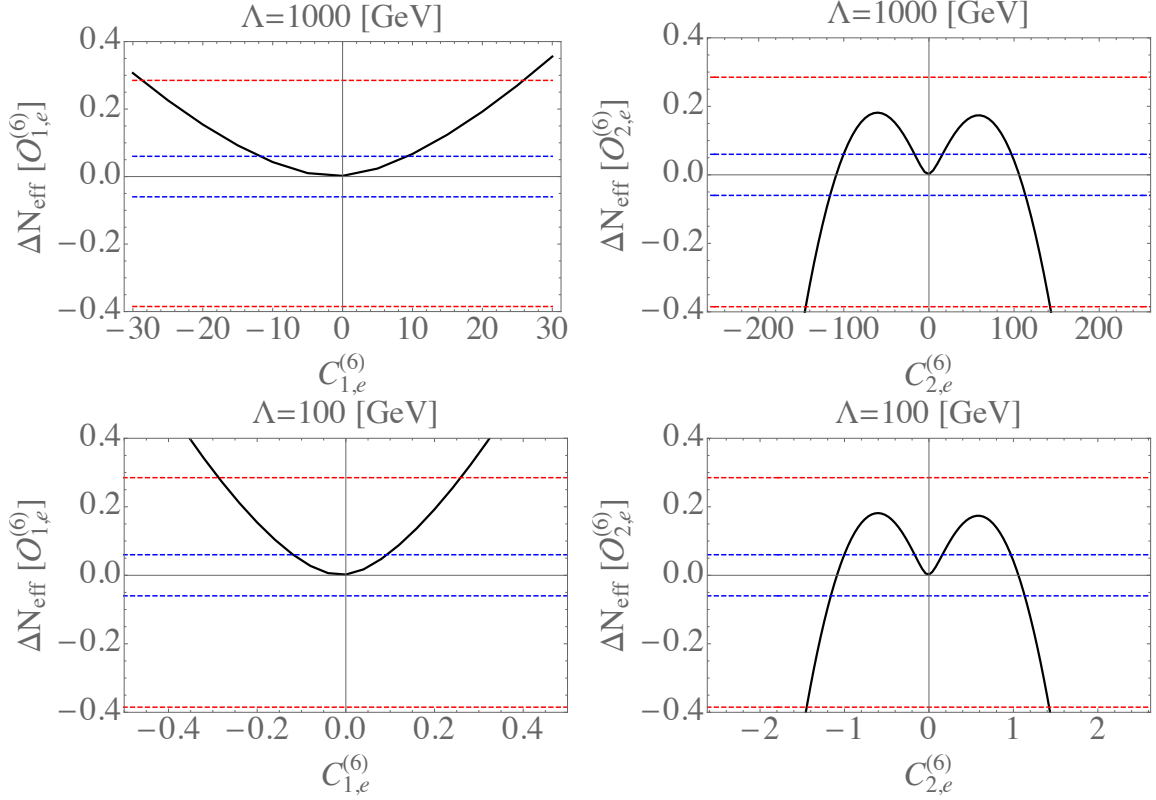


Figure 3. Corrections to N_{eff} from varying Wilson coefficients with $\Lambda = 1 \text{ TeV}$ and by considering only one non-vanishing NSI operator at a time. The upper left (right) panel corresponds to ΔN_{eff} from $\mathcal{O}_{1(2),e}^{(6)}$ with $\Lambda = 1000 \text{ GeV}$, and the lower left (right) panel is the same but with $\Lambda = 100 \text{ GeV}$. The black curve stands for corrections to N_{eff} from the NSI operator, and the horizontal colorful lines have the same meaning as those in figure 2. Note the scale difference of the horizontal axes and see more discussion in the main text.

- For $\Lambda = 1 \text{ TeV}$:

$$-28.7 \lesssim C_{1,e}^{(6)} \lesssim 25.8 \quad (\text{Planck}), \quad -11.8 \lesssim C_{1,e}^{(6)} \lesssim 9.0 \quad (\text{CMB-S4}) \quad (5.2)$$

$$-145.2 \lesssim C_{2,e}^{(6)} \lesssim 141.3 \quad (\text{Planck}), \quad -17.0 \lesssim C_{2,e}^{(6)} \lesssim 15.8 \quad (\text{CMB-S4}), \quad (5.3)$$

except for $C_{2,e}^{(6)} \in (-116.7, -100.7) \cup (96.4, 112.5)$ for CMB-S4.

- For $\Lambda = 100 \text{ GeV}$:

$$-0.29 \lesssim C_{1,e}^{(6)} \lesssim 0.26 \quad (\text{Planck}), \quad -0.12 \lesssim C_{1,e}^{(6)} \lesssim 0.09 \quad (\text{CMB-S4}) \quad (5.4)$$

$$-1.45 \lesssim C_{2,e}^{(6)} \lesssim 1.42 \quad (\text{Planck}), \quad -0.18 \lesssim C_{2,e}^{(6)} \lesssim 0.15 \quad (\text{CMB-S4}), \quad (5.5)$$

except for $C_{2,e}^{(6)} \in (-1.17, -1.01) \cup (0.96, 1.13)$ for CMB-S4.

For $C_{2,e}^{(6)}$, the two exception intervals for CMB-S4 in the last line of the two bullets above result from destructive interference as already discussed in last subsection — For $C_{2,e}^{(6)}$ of

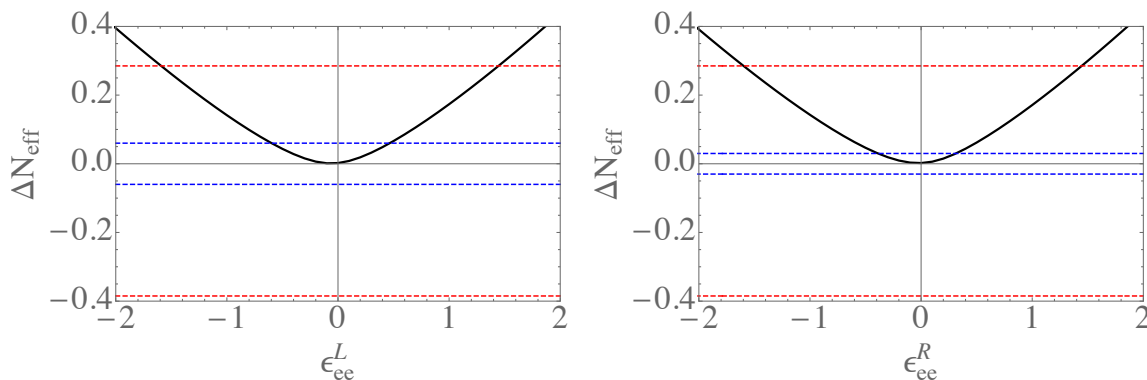


Figure 4. Constraints on $\epsilon_{e,L}$ (left panel) and $\epsilon_{e,R}$ (right panel) from N_{eff} . The black curves stand for corrections to N_{eff} from the dimension-6 NC NSI operators, and the colorful lines are the same as those in figure 2. See more details on the notations used in these two plots.

$\mathcal{O}(10)$ or larger, $\mathcal{O}_{1,e}^{(6)}$ is effectively of the weak scale, leading to the destructive interference and thus the two intervals. This can be understood more explicitly from the analytical expressions of the neutrino total energy densities from $\mathcal{O}_{1,e}^{(6)}$ and $\mathcal{O}_{2,e}^{(6)}$.¹⁵

$$\rho_{\nu\text{-total}}^{\text{interf.}}(\mathcal{O}_{1,e}^{(6)}) \simeq + \frac{256\sqrt{2}C_{1,e}^{(6)}G_F \sin^2 \theta_W T_\gamma^9}{\pi^5 \Lambda^2}, \quad (5.6)$$

$$\rho_{\nu\text{-total}}^{\text{interf.}}(\mathcal{O}_{2,e}^{(6)}) \simeq - \frac{40\sqrt{2}C_{2,e}^{(6)}G_F T_\gamma^5 T_{\nu_e}^4}{\pi^5 \Lambda^2} \times (1 + 4 \sin^2 \theta_W), \quad (5.7)$$

where θ_W is the weak mixing angle and we only show the interfering terms here by omitting any sub-leading effects in them in each case. Note that a larger (smaller) neutrino energy density would be equivalent to a higher (lower) neutrino temperature. Thus, as can be understood from eq. (2.3), the constructive (destructive) interference also explains the positive (negative) shift feature of N_{eff} from $\mathcal{O}_{1,e}^{(6)}$ ($\mathcal{O}_{2,e}^{(6)}$) in figures 2 and 3 when $\Lambda \sim \Lambda_W$. For the other NSI operators not shown in figure 3, since they are at least suppressed by one more power of Λ , Planck and CMB-S4 are not able to constrain those Wilson coefficients when Λ is fixed at 1 TeV. Similar observation is obtained for $\Lambda = 100$ GeV, with stronger constraints on $C_{1,e}^{(6)}$ and $C_{2,e}^{(6)}$, whose magnitudes are 100 times smaller compared with the $\Lambda = 1$ TeV case as expected.

5.3 Comparison with current constraints on NC NSIs

To compare with constraints on the dimension-6 operators $\mathcal{O}_{1(2),e}^{(6)}$ from other experiments, we first review the parameterization commonly used in the literatures to describe neutrino NSIs:

$$\mathcal{L}_{\text{NSI}}^{\text{NC}} = -2\sqrt{2}G_F \sum_{\alpha,\beta,f,P} \epsilon_{\alpha\beta}^{f,P} (\bar{\nu}_\alpha \gamma_\mu P_L \nu_\beta) (\bar{f} \gamma^\mu P f), \quad (5.8)$$

with $f = e, u, d$ the charged fermions, $\alpha, \beta = e, \mu, \tau$ the flavor of neutrinos, and $P = L, R$ the chiral projector operators where $L = (1 - \gamma_5)/2$ and $R = (1 + \gamma_5)/2$. Note that the nine

¹⁵These results can be readily obtained by using our completely dictionary in section 4.4 or the analytical expressions in the supplementary material as a `Mathematica` notebook file.

$\epsilon_{\alpha\beta}^{f,P}$'s are all real, and Hermiticity of the Lagrangian guarantees that only six of them are independent. The relevant operators for our study in this work are $\epsilon_{\alpha\beta}^{e,P}$. One readily finds, in terms of the Wilson coefficients used in this work, the ϵ parameters can be expressed as

$$\epsilon_{\alpha\beta}^{e,L} = \frac{C_{1,e}^{(6)} - C_{2,e}^{(6)}}{\Lambda^2 \cdot 2\sqrt{2}G_F}, \quad \epsilon_{\alpha\beta}^{e,R} = \frac{C_{1,e}^{(6)} + C_{2,e}^{(6)}}{\Lambda^2 \cdot 2\sqrt{2}G_F}. \quad (5.9)$$

Fixing $\Lambda \simeq 174.10$ GeV from the $\Lambda^2 \cdot 2\sqrt{2}G_F = 1$ condition such that the LEFT in our notation mimics that in eq. (5.8), we present our results for $\epsilon_{\alpha\beta}^{L,R}$ in figure 4 by including all NC NSIs in eq. (5.8) while ignoring all neutrino flavor dependence of $C_{(1,2),e}^{(6)}$. The colors in each subgraph of figure 4 have exactly the same meaning as those in figure 2, and to obtain the constraints, we once again ignore the neutrino flavor dependence of the LEFT Wilson coefficients and consider only one non-vanishing ϵ at a time in our analysis. However, we stress that, as one can see directly from eq. (5.9), one non-vanishing ϵ in general includes contributions from both $\mathcal{O}_{1,e}^{(6)}$ and $\mathcal{O}_{2,e}^{(6)}$. To summarize, we find the ϵ 's are constrained by N_{eff} as¹⁶

$$-1.60 \lesssim \epsilon^{e,L} \lesssim 1.44 \quad (\text{Planck}), \quad -0.61 \lesssim \epsilon^{e,L} \lesssim 0.46 \quad (\text{CMB-S4}); \quad (5.10)$$

$$-1.60 \lesssim \epsilon^{e,R} \lesssim 1.44 \quad (\text{Planck}), \quad -0.39 \lesssim \epsilon^{e,R} \lesssim 0.31 \quad (\text{CMB-S4}). \quad (5.11)$$

In comparison, we list constraints on these ϵ parameters from previous studies and ours obtained in this work in table 4 by ignoring bounds from loops [24, 94]. Note that constraints from ref. [106] in the second column are originally presented in terms of $\epsilon_{\alpha\beta}^{e,L+R} \equiv \epsilon_{\alpha\beta}^{e,L} + \epsilon_{\alpha\beta}^{e,R}$. We translate them on individual $\epsilon_{\alpha\beta}^{e,L(R)}$ by assuming only one of them non-vanishing. Constraints from TEXONO are obtained at the Kuo-Sheng Nuclear Power Station in ref. [100], the LEP, LSND and CHARM-II experiments in ref. [24], a global analysis of $\nu_e e$ and $\bar{\nu}_e e$ scattering data from LSND, Irvine, Rovno and MUNU experiments in ref. [86], a combination of OPAL, ALEPH, L3, DELPHI, LSND, CHARM-II, Irvine, Rovno and MUNU experiments in ref. [87], solar and reactor neutrino experiments in ref. [88], low-energy solar neutrinos at source and detector from the Borexino experiment in ref. [93], a global analysis of short baseline νe and $\bar{\nu} e$ data from LSND, LAMPF, Irvine, Rovno, MUNU, TEXONO and KRANOYARSK in ref. [101], and the DUNE experiment in ref. [39]. For constraints from ref. [86], we cite their results in the one-parameter case since it leads to the most stringent constraints on these NC NSIs, and similarly for results in refs. [93, 101]. For constraints from ref. [39], the upper and the lower intervals are obtained using an exposure of 300 and 850 kt.MW.yr for DUNE respectively. For constraints from ref. [93], the upper number is obtained from a detector-only study using low-energy solar neutrinos at Borexino, while the lower is the future prospect from a combined analysis of the detector and the source. For all the other cases in table 4, whenever two intervals appear, it means two “disjoint” ranges that are simultaneously allowed from their analyses. We refer the reader to the original references for more details.

¹⁶Since we ignore the neutrino flavor dependence, we thus leave out the neutrino flavor indices here and in the following.

ϵ 's	[106]	[100]	[24]	[86]	[87]	[88]	[93]	[101]	[39]	This work	
										Planck	CMB-S4
$\epsilon_{ee}^{e,L}$	[-0.010, 2.039]	[-1.53, 0.38]	[-0.07, 0.1]	[-0.05, 0.12]	[-0.03, 0.08]	[-0.036, 0.063]	[-0.017, 0.027] [-0.003, 0.003]	[-0.08, 0.08]	[-0.185, 0.380] [-0.130, 0.185]	[-1.6, 1.44]	[-0.61, 0.46]
$\epsilon_{\mu\mu}^{e,L}$	[-0.179, 0.146]	[-0.84, 0.84]	—	—	[-0.13, 0.13]	—	[-0.152, 0.152] [-0.055, 0.055]	[-0.33, 0.35]	[-0.025, 0.052] [-0.017, 0.040]	[-1.6, 1.44]	[-0.61, 0.46]
$\epsilon_{\tau\tau}^{e,L}$	[-0.860, 0.350]	[-0.84, 0.84]	[-0.4, 0.4]	[-0.44, 0.44]	[-0.33, 0.33]	—	[-0.152, 0.152] [-0.055, 0.055]	[-0.33, 0.35]	[-0.055, 0.023] [-0.042, 0.012]	[-1.6, 1.44]	[-0.61, 0.46]
$\epsilon_{\mu\mu}^{e,L}$	[-0.364, 1.387]	—	[-0.03, 0.03]	—	[-0.03, 0.03]	—	[-0.040, 0.04] [-0.010, 0.010]	—	[-0.290, 0.390] [-0.192, 0.240]	[-1.6, 1.44]	[-0.61, 0.46]
$\epsilon_{\mu\tau}^{e,L}$	[-0.035, 0.028]	—	[-0.1, 0.1]	—	[-0.1, 0.1]	—	—	—	[-0.015, 0.013] [-0.010, 0.010]	[-1.6, 1.44]	[-0.61, 0.46]
$\epsilon_{\tau\tau}^{e,L}$	[-0.350, 1.400]	—	[-0.5, 0.5]	—	[-0.46, 0.24]	[-0.16, 0.110] [0.41, 0.66]	[-0.040, 0.04] [-0.010, 0.010]	—	[-0.360, 0.145] [-0.120, 0.095]	[-1.6, 1.44]	[-0.61, 0.46]
$\epsilon_{ee}^{e,R}$	[-0.010, 2.039]	[-0.07, 0.08]	[-1, 0.5]	[-0.04, 0.14]	[0.004, 0.151]	[-0.27, 0.59]	[-0.33, 0.25] [-0.07, 0.07]	[-0.04, 0.06]	[-0.185, 0.380] [-0.130, 0.185]	[-1.6, 1.44]	[-0.39, 0.31]
$\epsilon_{\mu\mu}^{e,R}$	[-0.179, 0.146]	[-0.19, 0.19]	—	—	[-0.13, 0.13]	—	[-0.236, 0.236] [-0.08, 0.08]	[-0.15, 0.16]	[-0.025, 0.052] [-0.017, 0.040]	[-1.6, 1.44]	[-0.39, 0.31]
$\epsilon_{\tau\tau}^{e,R}$	[-0.860, 0.350]	[-0.19, 0.19]	[-0.7, 0.7]	[-0.27, 0.27]	[-0.05, 0.05] [-0.28, 0.28]	—	[-0.236, 0.236] [-0.08, 0.08]	[-0.15, 0.16]	[-0.055, 0.023] [-0.042, 0.012]	[-1.6, 1.44]	[-0.39, 0.31]
$\epsilon_{\mu\mu}^{e,R}$	[-0.364, 1.387]	—	[-0.03, 0.03]	—	[-0.03, 0.03]	—	[-0.10, 0.12] [-0.006, 0.006]	—	[-0.290, 0.390] [-0.192, 0.240]	[-1.6, 1.44]	[-0.39, 0.31]
$\epsilon_{\mu\tau}^{e,R}$	[-0.035, 0.028]	—	[-0.1, 0.1]	—	[-0.1, 0.1]	—	—	—	[-0.015, 0.013] [-0.010, 0.010]	[-1.6, 1.44]	[-0.39, 0.31]
$\epsilon_{\tau\tau}^{e,R}$	[-0.350, 1.400]	—	[-0.5, 0.5]	—	[-0.25, 0.43]	[-1.05, 0.31]	[-0.10, 0.12] [-0.006, 0.006]	—	[-0.360, 0.145] [-0.120, 0.095]	[-1.6, 1.44]	[-0.39, 0.31]

Table 4. Summary of constraints on dimension-6 neutrino-electron NC NSIs from previous studies and this work. Constraints from a global fitting of all kinds of neutrino oscillation data plus the COHERENT result are obtained in ref. [106], the TEXONO collaboration in ref. [100], the LEP, LSND and CHARM-II experiments in ref. [24], a global analysis of $\nu_e e$ and $\bar{\nu}_e e$ scattering data from LSND, Irvine, Rovno and MUNU experiments in ref. [86], OPAL, ALEPH, L3, DELPHI, LSND, CHARM-II, Irvine, Rovno and MUNU experiments in ref. [87], solar and reactor neutrino experiments in ref. [88], low-energy solar neutrinos at source and detector from the Borexino experiment in ref. [93], a global analysis of short baseline νe and $\bar{\nu} e$ data from LSND, LAMPF, Irvine, Rovno, MUNU, TEXONO and KRANOYARSK in ref. [101], and DUNE in ref. [39].

As one can see from table 4, in general, constraints from other experiments are stronger than those we obtain from Planck. However, from the last column of table 4, the results from CMB-S4 would be improved by a factor of ~ 3 (5) for $\epsilon^{e,L(R)}$. As a result, all the ϵ 's would be bounded at the 10% level. On the other hand, in table 4, one notes that seven of these ϵ 's are constrained at the 10% level from previous experiments, except the following five's: $\epsilon_{ee}^{e,L}$ [87, 88], $\epsilon_{\mu\mu}^{e,(L,R)}$ [24, 87], $\epsilon_{\mu\tau}^{e,L}$ [106], $\epsilon_{ee}^{e,R}$ [100], and $\epsilon_{\mu\tau}^{e,R}$ [106] that are stringently constrained at the 1% level. Therefore, constraints on most of these ϵ 's from CMB-S4 are basically comparable to the existing ones. For example, $\epsilon_{\tau\tau}^{e,R}$ is constrained to be [-0.25, 0.43] in ref. [87] from the OPAL, ALEPH, L3, DELPHI, LSND, CHARM-II, Irvine, Rovno and MUNU experiments, while it would be [-0.39, 0.31] from CMB-S4. Furthermore, we point out that, in the four-parameter cases of ref. [86], our results for $\epsilon^{e,R}$ from CMB-S4 are slightly stronger than theirs. Similarly, in the two-parameter (correlated) case, our constraints on $\epsilon_{\mu\mu,ee}^{e,R}$ ($\epsilon_{e\mu,e\tau}^{e,L}$) are stronger than those obtained in ref. [93] ([101]), while weaker or comparable to theirs for the other ϵ 's.

On the other hand, taking both $\epsilon^{e,L}$ and $\epsilon^{e,R}$ into account, we obtain simultaneous constraints on $\epsilon^{e,L}$ and $\epsilon^{e,R}$ as shown in figure 5, where the orange and the purple regions are still allowed by Planck and CMB-S4 respectively. The permitted regions are along

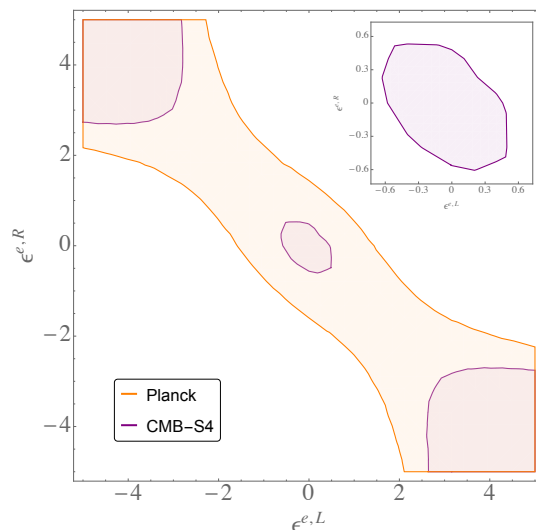


Figure 5. Simultaneous constraints on $\epsilon_{e,L}$ and $\epsilon_{e,R}$ from precision measurements of N_{eff} from Planck and CMB-S4. The allowed regions are indicated by the orange and the purple respectively. The subgraph in the upper right corner corresponds to the magnified allowed region from CMB-S4 near the origin. See the main text for a detailed discussion.

the diagonal region on the $\epsilon_{e,L}-\epsilon_{e,R}$ plane since it is where contributions from $\mathcal{O}_{1,e}^{(6)}$ and $\mathcal{O}_{2,e}^{(6)}$ cancel. This effect becomes more evident when the magnitudes of $\epsilon^{e,L}$ and $\epsilon^{e,R}$ are large, as implied by the purple regions when $|\epsilon^{e,(L,R)}| \gtrsim 4$. The subfigure in the upper right corner of figure 5 is the enlarged allowed region from CMB-S4 near the origin. Since we assume neutrino flavor independence and N_{eff} is more sensitive to light degrees of freedom, our constraints are slightly less stringent than, but again very comparable to, those discussed in last paragraph. Our results presented in this work complement those from previous studies on NC neutrino NSIs from collider, neutrino coherent scattering and neutrino oscillation experiments.

6 Conclusions

Null observation of any new resonances after the discovery of the Higgs particle at the LHC has gradually changed our strategy in searching for new physics from specific UV models to model-independent studies. EFTs provide a systematic and model independent approach to heavy new physics. In the early Universe where the active fields are neutrinos, electrons, positrons and photons, the system can be described by the LEFT, even with the introduction of some new physics above the $\sim \mathcal{O}(100 \text{ MeV})$ scale. NC NSIs induced by the new physics would affect neutrino decoupling in the early Universe, thus would also modify the prediction of N_{eff} . In light of the very precision measurements of N_{eff} from current Planck data and the precision target from CMB-S4, we present constraints on NC NSIs from N_{eff} up to dimension-7 in this work by assuming that all NC NSIs are induced by heavy mediators above $\sim \mathcal{O}(100 \text{ MeV})$.

To that end, we adopt the strategy developed in refs. [124, 125], which permits a fast and precision calculation of N_{eff} , and can also be easily generalized to include various new physics. The fast calculation of N_{eff} largely seeds in the pre-calculated collision term integrals, which are only obtained for several specific processes in the SM. In this work, we provide a complete, generic and analytical dictionary for these collision term integrals in section 4. With our results, as long as the invariant amplitudes are known, one can refer to this dictionary to write down the Boltzmann equations, and then solve the prediction of N_{eff} from the SM or some new physics with few efforts. We also show an example for the application of this dictionary at the end of section 4.

Including the NC NSIs and using the dictionary described above, we study constraints on these operators from precision measurements of N_{eff} . Our results are presented in figure 1 and summarized in table 3, where the lower bounds on the scale of new physics Λ is obtained by fixing the Wilson coefficients at unity and considering only one non-vanishing NSI operator at a time. We find that, the dimension-6 NSI operators $\mathcal{O}_{1,e}^{(6)}$ and $\mathcal{O}_{2,e}^{(6)}$ are constrained to be above ~ 331 GeV and ~ 240 GeV respectively from CMB-S4. On the other hand, due to suppression from the new physics scale, the couplings and m_e , dimension-7 operators $\mathcal{O}_{(5,6,7,8,9,10,11),e}^{(7)}$ only have visible corrections to N_{eff} when the new physics is relatively light, thus the current lower bounds on these operators are about 6 GeV and 3 GeV for $\mathcal{O}_{(7,8,9,10,11),e}^{(7)}$ and $\mathcal{O}_{(5,6),e}^{(7)}$, respectively. Operators $\mathcal{O}_{3,4,5}^{(6)}$ are not constrained from N_{eff} due to (1) negligible corrections to N_{eff} when $\Lambda \gtrsim \Lambda_W$ and (2) realization of thermal equilibrium among the three flavor neutrinos that results in vanishing contributions to N_{eff} . Operators $\mathcal{O}_{(1,2),e}^{(7)}$ are also not constrained from N_{eff} due to suppression of tiny couplings.

On the other hand, we also study constraints on the Wilson coefficients with Λ fixed at 1 TeV and 100 GeV. The results are shown in figure 3 by taking only one non-vanishing NSI operator into account at a time. We find that only $C_{1,e}^{(6)}$ and $C_{2,e}^{(6)}$ are constrained by N_{eff} since the dimension-7 operators are all suppressed by one more power of Λ , as well as m_e and the small couplings. At $\Lambda = 100$ GeV, we find the magnitude of $C_{1,e}^{(6)}$ is constrained to be around 0.3 (0.1) from Planck (CMB-S4), while it is about 1.4 (0.2) for $C_{2,e}^{(6)}$ from Planck (CMB-S4). The results are summarized in eqs. (5.2)–(5.5).

Constraints on the dimension-6 neutrino-electron NC NSI operators $\mathcal{O}_{(1,2),e}^{(6)}$ from precision measurements of N_{eff} are also compared with previous results from, for example, a global fitting of neutrino oscillation experiments and collider experiments. To that end, we first obtain constraints on the NC NSIs using the ϵ parameterization, and then present the results in figure 4 and table 4 for one non-vanishing NC NSI operator at a time, and figure 5 for the inclusion of both operators. We find that constraints from precision measurements of N_{eff} from Planck are in general weaker than those from other experiments mentioned above. However, the improved results from CMB-S4 in future would become comparable for certain operators. Our work complements previous studies on NC NSIs from other experiments. In the future, if the cosmic neutrino background ($C\nu B$) could be directly measured, N_{eff} would be determined with a much better precision, and one could then expect also much stronger constraints on these NC neutrino NSIs from $C\nu B$.

Acknowledgments

We thank Shu-Yuan Guo for his valuable contribution at the early stage of this project, Miguel Escudero for helpful discussion, and the HPC Cluster of ITP-CAS for the computation support. YD and JHY were supported by the National Science Foundation of China (NSFC) under Grants No. 12022514 and No. 11875003. JHY was also supported by the National Science Foundation of China (NSFC) under Grants No. 12047503 and National Key Research and Development Program of China Grant No. 2020YFC2201501.

Open Access. This article is distributed under the terms of the Creative Commons Attribution License ([CC-BY 4.0](https://creativecommons.org/licenses/by/4.0/)), which permits any use, distribution and reproduction in any medium, provided the original author(s) and source are credited.

References

- [1] ATLAS collaboration, *Observation of a new particle in the search for the Standard Model Higgs boson with the ATLAS detector at the LHC*, *Phys. Lett. B* **716** (2012) 1 [[arXiv:1207.7214](https://arxiv.org/abs/1207.7214)] [[INSPIRE](#)].
- [2] CMS collaboration, *Observation of a new boson at a mass of 125 GeV with the CMS experiment at the LHC*, *Phys. Lett. B* **716** (2012) 30 [[arXiv:1207.7235](https://arxiv.org/abs/1207.7235)] [[INSPIRE](#)].
- [3] S. Weinberg, *Baryon and lepton nonconserving processes*, *Phys. Rev. Lett.* **43** (1979) 1566 [[INSPIRE](#)].
- [4] W. Buchmüller and D. Wyler, *Effective Lagrangian analysis of new interactions and flavor conservation*, *Nucl. Phys. B* **268** (1986) 621 [[INSPIRE](#)].
- [5] B. Grzadkowski, M. Iskrzynski, M. Misiak and J. Rosiek, *Dimension-six terms in the Standard Model Lagrangian*, *JHEP* **10** (2010) 085 [[arXiv:1008.4884](https://arxiv.org/abs/1008.4884)] [[INSPIRE](#)].
- [6] L. Lehman, *Extending the Standard Model effective field theory with the complete set of dimension-7 operators*, *Phys. Rev. D* **90** (2014) 125023 [[arXiv:1410.4193](https://arxiv.org/abs/1410.4193)] [[INSPIRE](#)].
- [7] H.-L. Li, Z. Ren, J. Shu, M.-L. Xiao, J.-H. Yu and Y.-H. Zheng, *Complete set of dimension-8 operators in the Standard Model effective field theory*, [arXiv:2005.00008](https://arxiv.org/abs/2005.00008) [[INSPIRE](#)].
- [8] C.W. Murphy, *Dimension-8 operators in the Standard Model effective field theory*, *JHEP* **10** (2020) 174 [[arXiv:2005.00059](https://arxiv.org/abs/2005.00059)] [[INSPIRE](#)].
- [9] H.-L. Li, Z. Ren, M.-L. Xiao, J.-H. Yu and Y.-H. Zheng, *Complete set of dimension-9 operators in the Standard Model effective field theory*, [arXiv:2007.07899](https://arxiv.org/abs/2007.07899) [[INSPIRE](#)].
- [10] Y. Liao and X.-D. Ma, *An explicit construction of the dimension-9 operator basis in the Standard Model effective field theory*, *JHEP* **11** (2020) 152 [[arXiv:2007.08125](https://arxiv.org/abs/2007.08125)] [[INSPIRE](#)].
- [11] Y. Liao and X.-D. Ma, *Renormalization group evolution of dimension-seven baryon- and lepton-number-violating operators*, *JHEP* **11** (2016) 043 [[arXiv:1607.07309](https://arxiv.org/abs/1607.07309)] [[INSPIRE](#)].
- [12] E.E. Jenkins, A.V. Manohar and P. Stoffer, *Low-energy effective field theory below the electroweak scale: operators and matching*, *JHEP* **03** (2018) 016 [[arXiv:1709.04486](https://arxiv.org/abs/1709.04486)] [[INSPIRE](#)].

- [13] Y. Liao, X.-D. Ma and Q.-Y. Wang, *Extending low energy effective field theory with a complete set of dimension-7 operators*, *JHEP* **08** (2020) 162 [[arXiv:2005.08013](#)] [[INSPIRE](#)].
- [14] H.-L. Li, Z. Ren, M.-L. Xiao, J.-H. Yu and Y.-H. Zheng, *Low energy effective field theory operator basis at $d \leq 9$* , [arXiv:2012.09188](#) [[INSPIRE](#)].
- [15] C.W. Murphy, *Low-energy effective field theory below the electroweak scale: dimension-8 operators*, *JHEP* **04** (2021) 101 [[arXiv:2012.13291](#)] [[INSPIRE](#)].
- [16] R. Davis, Jr., D.S. Harmer and K.C. Hoffman, *Search for neutrinos from the sun*, *Phys. Rev. Lett.* **20** (1968) 1205 [[INSPIRE](#)].
- [17] SNO collaboration, *Measurement of the rate of $\nu_e + d \rightarrow p + p + e^-$ interactions produced by 8B solar neutrinos at the Sudbury Neutrino Observatory*, *Phys. Rev. Lett.* **87** (2001) 071301 [[nucl-ex/0106015](#)] [[INSPIRE](#)].
- [18] SUPER-KAMIOKANDE collaboration, *Evidence for oscillation of atmospheric neutrinos*, *Phys. Rev. Lett.* **81** (1998) 1562 [[hep-ex/9807003](#)] [[INSPIRE](#)].
- [19] DAYA BAY collaboration, *Observation of electron-antineutrino disappearance at Daya Bay*, *Phys. Rev. Lett.* **108** (2012) 171803 [[arXiv:1203.1669](#)] [[INSPIRE](#)].
- [20] K2K collaboration, *Indications of neutrino oscillation in a 250 km long baseline experiment*, *Phys. Rev. Lett.* **90** (2003) 041801 [[hep-ex/0212007](#)] [[INSPIRE](#)].
- [21] MINOS collaboration, *Observation of muon neutrino disappearance with the MINOS detectors and the NuMI neutrino beam*, *Phys. Rev. Lett.* **97** (2006) 191801 [[hep-ex/0607088](#)] [[INSPIRE](#)].
- [22] L. Wolfenstein, *Neutrino oscillations in matter*, *Phys. Rev. D* **17** (1978) 2369 [[INSPIRE](#)].
- [23] S.P. Mikheyev and A.Y. Smirnov, *Resonance amplification of oscillations in matter and spectroscopy of solar neutrinos*, *Sov. J. Nucl. Phys.* **42** (1985) 913 [*Yad. Fiz.* **42** (1985) 1441] [[INSPIRE](#)].
- [24] S. Davidson, C. Pena-Garay, N. Rius and A. Santamaria, *Present and future bounds on nonstandard neutrino interactions*, *JHEP* **03** (2003) 011 [[hep-ph/0302093](#)] [[INSPIRE](#)].
- [25] T. Ohlsson, *Status of non-standard neutrino interactions*, *Rept. Prog. Phys.* **76** (2013) 044201 [[arXiv:1209.2710](#)] [[INSPIRE](#)].
- [26] Y. Farzan and M. Tortola, *Neutrino oscillations and non-standard interactions*, *Front. in Phys.* **6** (2018) 10 [[arXiv:1710.09360](#)] [[INSPIRE](#)].
- [27] *Neutrino non-standard interactions: a status report*, *SciPost Phys. Proc.* **2** (2019) 001 [[arXiv:1907.00991](#)] [[INSPIRE](#)].
- [28] K.N. Abazajian et al., *Light sterile neutrinos: a white paper*, [arXiv:1204.5379](#) [[INSPIRE](#)].
- [29] P. Agrawal and V. Rentala, *Identifying dark matter interactions in monojet searches*, *JHEP* **05** (2014) 098 [[arXiv:1312.5325](#)] [[INSPIRE](#)].
- [30] A. Nelson, L.M. Carpenter, R. Cotta, A. Johnstone and D. Whiteson, *Confronting the Fermi line with LHC data: an effective theory of dark matter interaction with photons*, *Phys. Rev. D* **89** (2014) 056011 [[arXiv:1307.5064](#)] [[INSPIRE](#)].
- [31] F. Pobbe, A. Wulzer and M. Zanetti, *Setting limits on effective field theories: the case of dark matter*, *JHEP* **08** (2017) 074 [[arXiv:1704.00736](#)] [[INSPIRE](#)].

- [32] D. Choudhury, K. Ghosh and S. Niyogi, *Probing nonstandard neutrino interactions at the LHC run II*, *Phys. Lett. B* **784** (2018) 248 [[arXiv:1801.01513](#)] [[INSPIRE](#)].
- [33] A. Friedland, M.L. Graesser, I.M. Shoemaker and L. Vecchi, *Probing nonstandard Standard Model backgrounds with LHC monojets*, *Phys. Lett. B* **714** (2012) 267 [[arXiv:1111.5331](#)] [[INSPIRE](#)].
- [34] K.S. Babu, D. Gonçalves, S. Jana and P.A.N. Machado, *Neutrino non-standard interactions: complementarity between LHC and oscillation experiments*, *Phys. Lett. B* **815** (2021) 136131 [[arXiv:2003.03383](#)] [[INSPIRE](#)].
- [35] A. Falkowski, M. González-Alonso and K. Mimouni, *Compilation of low-energy constraints on 4-fermion operators in the SMEFT*, *JHEP* **08** (2017) 123 [[arXiv:1706.03783](#)] [[INSPIRE](#)].
- [36] F.J. Escrihuela, M. Tortola, J.W.F. Valle and O.G. Miranda, *Global constraints on muon-neutrino non-standard interactions*, *Phys. Rev. D* **83** (2011) 093002 [[arXiv:1103.1366](#)] [[INSPIRE](#)].
- [37] P. Coloma, M.C. Gonzalez-Garcia, M. Maltoni and T. Schwetz, *COHERENT enlightenment of the neutrino dark side*, *Phys. Rev. D* **96** (2017) 115007 [[arXiv:1708.02899](#)] [[INSPIRE](#)].
- [38] W. Altmannshofer, M. Tammaro and J. Zupan, *Non-standard neutrino interactions and low energy experiments*, *JHEP* **09** (2019) 083 [[arXiv:1812.02778](#)] [[INSPIRE](#)].
- [39] K.S. Babu, P.S.B. Dev, S. Jana and A. Thapa, *Non-standard interactions in radiative neutrino mass models*, *JHEP* **03** (2020) 006 [[arXiv:1907.09498](#)] [[INSPIRE](#)].
- [40] A.N. Khan and W. Rodejohann, *New physics from COHERENT data with an improved quenching factor*, *Phys. Rev. D* **100** (2019) 113003 [[arXiv:1907.12444](#)] [[INSPIRE](#)].
- [41] D.K. Papoulias, T.S. Kosmas and Y. Kuno, *Recent probes of standard and non-standard neutrino physics with nuclei*, *Front. in Phys.* **7** (2019) 191 [[arXiv:1911.00916](#)] [[INSPIRE](#)].
- [42] B.C. Canas, E.A. Garcés, O.G. Miranda, A. Parada and G. Sanchez Garcia, *Interplay between nonstandard and nuclear constraints in coherent elastic neutrino-nucleus scattering experiments*, *Phys. Rev. D* **101** (2020) 035012 [[arXiv:1911.09831](#)] [[INSPIRE](#)].
- [43] A. Falkowski, M. González-Alonso and Z. Tabrizi, *Reactor neutrino oscillations as constraints on effective field theory*, *JHEP* **05** (2019) 173 [[arXiv:1901.04553](#)] [[INSPIRE](#)].
- [44] OPAL collaboration, *Tests of the Standard Model and constraints on new physics from measurements of fermion pair production at 189 GeV to 209 GeV at LEP*, *Eur. Phys. J. C* **33** (2004) 173 [[hep-ex/0309053](#)] [[INSPIRE](#)].
- [45] ZEUS collaboration, *Search for contact interactions in deep inelastic $e^+p \rightarrow e^+X$ scattering at HERA*, *Eur. Phys. J. C* **14** (2000) 239 [[hep-ex/9905039](#)] [[INSPIRE](#)].
- [46] H1 collaboration, *Search for compositeness, leptoquarks and large extra dimensions in eq contact interactions at HERA*, *Phys. Lett. B* **479** (2000) 358 [[hep-ex/0003002](#)] [[INSPIRE](#)].
- [47] CMS collaboration, *Search for dark matter, extra dimensions, and unparticles in monojet events in proton-proton collisions at $\sqrt{s} = 8$ TeV*, *Eur. Phys. J. C* **75** (2015) 235 [[arXiv:1408.3583](#)] [[INSPIRE](#)].
- [48] ATLAS collaboration, *Search for new phenomena in final states with an energetic jet and large missing transverse momentum in pp collisions at $\sqrt{s} = 8$ TeV with the ATLAS detector*, *Eur. Phys. J. C* **75** (2015) 299 [Erratum *ibid.* **75** (2015) 408] [[arXiv:1502.01518](#)] [[INSPIRE](#)].

- [49] I. Doršner, S. Fajfer, A. Greljo, J.F. Kamenik and N. Košnik, *Physics of leptoquarks in precision experiments and at particle colliders*, *Phys. Rept.* **641** (2016) 1 [[arXiv:1603.04993](#)] [[INSPIRE](#)].
- [50] M.B. Wise and Y. Zhang, *Effective theory and simple completions for neutrino interactions*, *Phys. Rev. D* **90** (2014) 053005 [[arXiv:1404.4663](#)] [[INSPIRE](#)].
- [51] M. Lindner, W. Rodejohann and X.-J. Xu, *Coherent neutrino-nucleus scattering and new neutrino interactions*, *JHEP* **03** (2017) 097 [[arXiv:1612.04150](#)] [[INSPIRE](#)].
- [52] W. Rodejohann, X.-J. Xu and C.E. Yaguna, *Distinguishing between Dirac and Majorana neutrinos in the presence of general interactions*, *JHEP* **05** (2017) 024 [[arXiv:1702.05721](#)] [[INSPIRE](#)].
- [53] I. Bischer and W. Rodejohann, *General neutrino interactions at the DUNE near detector*, *Phys. Rev. D* **99** (2019) 036006 [[arXiv:1810.02220](#)] [[INSPIRE](#)].
- [54] I. Bischer and W. Rodejohann, *General neutrino interactions from an effective field theory perspective*, *Nucl. Phys. B* **947** (2019) 114746 [[arXiv:1905.08699](#)] [[INSPIRE](#)].
- [55] A.N. Khan, W. Rodejohann and X.-J. Xu, *Borexino and general neutrino interactions*, *Phys. Rev. D* **101** (2020) 055047 [[arXiv:1906.12102](#)] [[INSPIRE](#)].
- [56] C. Biggio, M. Blennow and E. Fernandez-Martinez, *General bounds on non-standard neutrino interactions*, *JHEP* **08** (2009) 090 [[arXiv:0907.0097](#)] [[INSPIRE](#)].
- [57] N. Cabibbo, *Unitary symmetry and leptonic decays*, *Phys. Rev. Lett.* **10** (1963) 531 [[INSPIRE](#)].
- [58] M. Kobayashi and T. Maskawa, *CP violation in the renormalizable theory of weak interaction*, *Prog. Theor. Phys.* **49** (1973) 652 [[INSPIRE](#)].
- [59] W. Loinaz, N. Okamura, S. Rayyan, T. Takeuchi and L.C.R. Wijewardhana, *The NuTeV anomaly, lepton universality, and nonuniversal neutrino gauge couplings*, *Phys. Rev. D* **70** (2004) 113004 [[hep-ph/0403306](#)] [[INSPIRE](#)].
- [60] KARMEN collaboration, *Latest results of the KARMEN2 experiment*, *Nucl. Phys. B Proc. Suppl.* **91** (2001) 191 [[hep-ex/0008002](#)] [[INSPIRE](#)].
- [61] NOMAD collaboration, *Final NOMAD results on $\nu_\mu \rightarrow \nu_\tau$ and $\nu_e \rightarrow \nu_\tau$ oscillations including a new search for ν_τ appearance using hadronic τ decays*, *Nucl. Phys. B* **611** (2001) 3 [[hep-ex/0106102](#)] [[INSPIRE](#)].
- [62] NOMAD collaboration, *Search for $\nu_\mu \rightarrow \nu_e$ oscillations in the NOMAD experiment*, *Phys. Lett. B* **570** (2003) 19 [[hep-ex/0306037](#)] [[INSPIRE](#)].
- [63] PARTICLE DATA GROUP collaboration, *Review of particle physics*, *PTEP* **2020** (2020) 083C01 [[INSPIRE](#)].
- [64] J. Terol-Calvo, M. Tórtola and A. Vicente, *High-energy constraints from low-energy neutrino nonstandard interactions*, *Phys. Rev. D* **101** (2020) 095010 [[arXiv:1912.09131](#)] [[INSPIRE](#)].
- [65] Y. Du, H.-L. Li, J. Tang, S. Vihonen and J.-H. Yu, *Non-standard interactions in SMEFT confronted with terrestrial neutrino experiments*, *JHEP* **03** (2021) 019 [[arXiv:2011.14292](#)] [[INSPIRE](#)].
- [66] R.J. Hill and O. Tomalak, *On the effective theory of neutrino-electron and neutrino-quark interactions*, *Phys. Lett. B* **805** (2020) 135466 [[arXiv:1911.01493](#)] [[INSPIRE](#)].

- [67] R. Harnik, J. Kopp and P.A.N. Machado, *Exploring ν signals in dark matter detectors*, *JCAP* **07** (2012) 026 [[arXiv:1202.6073](#)] [[INSPIRE](#)].
- [68] M. Cadeddu and F. Dordei, *Reinterpreting the weak mixing angle from atomic parity violation in view of the Cs neutron rms radius measurement from COHERENT*, *Phys. Rev. D* **99** (2019) 033010 [[arXiv:1808.10202](#)] [[INSPIRE](#)].
- [69] G.-Y. Huang and S. Zhou, *Constraining neutrino lifetimes and magnetic moments via solar neutrinos in the large Xenon detectors*, *JCAP* **02** (2019) 024 [[arXiv:1810.03877](#)] [[INSPIRE](#)].
- [70] I.M. Shoemaker and J. Wyenberg, *Direct detection experiments at the neutrino dipole portal frontier*, *Phys. Rev. D* **99** (2019) 075010 [[arXiv:1811.12435](#)] [[INSPIRE](#)].
- [71] D. Aristizabal Sierra, N. Rojas and M.H.G. Tytgat, *Neutrino non-standard interactions and dark matter searches with multi-ton scale detectors*, *JHEP* **03** (2018) 197 [[arXiv:1712.09667](#)] [[INSPIRE](#)].
- [72] M.C. Gonzalez-Garcia, M. Maltoni, Y.F. Perez-Gonzalez and R. Zukanovich Funchal, *Neutrino discovery limit of dark matter direct detection experiments in the presence of non-standard interactions*, *JHEP* **07** (2018) 019 [[arXiv:1803.03650](#)] [[INSPIRE](#)].
- [73] B. Dutta, S. Liao, L.E. Strigari and J.W. Walker, *Non-standard interactions of solar neutrinos in dark matter experiments*, *Phys. Lett. B* **773** (2017) 242 [[arXiv:1705.00661](#)] [[INSPIRE](#)].
- [74] E. Bertuzzo, F.F. Deppisch, S. Kulkarni, Y.F. Perez Gonzalez and R. Zukanovich Funchal, *Dark matter and exotic neutrino interactions in direct detection searches*, *JHEP* **04** (2017) 073 [[arXiv:1701.07443](#)] [[INSPIRE](#)].
- [75] J.B. Dent, B. Dutta, S. Liao, J.L. Newstead, L.E. Strigari and J.W. Walker, *Probing light mediators at ultralow threshold energies with coherent elastic neutrino-nucleus scattering*, *Phys. Rev. D* **96** (2017) 095007 [[arXiv:1612.06350](#)] [[INSPIRE](#)].
- [76] D.G. Cerdeño, M. Fairbairn, T. Jubb, P.A.N. Machado, A.C. Vincent and C. Boehm, *Physics from solar neutrinos in dark matter direct detection experiments*, *JHEP* **05** (2016) 118 [*Erratum ibid.* **09** (2016) 048] [[arXiv:1604.01025](#)] [[INSPIRE](#)].
- [77] P. Coloma, P. Huber and J.M. Link, *Combining dark matter detectors and electron-capture sources to hunt for new physics in the neutrino sector*, *JHEP* **11** (2014) 042 [[arXiv:1406.4914](#)] [[INSPIRE](#)].
- [78] M. Pospelov and J. Pradler, *Dark matter or neutrino recoil? Interpretation of recent experimental results*, *Phys. Rev. D* **89** (2014) 055012 [[arXiv:1311.5764](#)] [[INSPIRE](#)].
- [79] M. Pospelov and J. Pradler, *Elastic scattering signals of solar neutrinos with enhanced baryonic currents*, *Phys. Rev. D* **85** (2012) 113016 [*Erratum ibid.* **88** (2013) 039904] [[arXiv:1203.0545](#)] [[INSPIRE](#)].
- [80] J. Kopp, M. Lindner, T. Ota and J. Sato, *Non-standard neutrino interactions in reactor and superbeam experiments*, *Phys. Rev. D* **77** (2008) 013007 [[arXiv:0708.0152](#)] [[INSPIRE](#)].
- [81] D. Liu, C. Sun and J. Gao, *Constraints on neutrino non-standard interactions from LHC data with large missing transverse momentum*, *JHEP* **02** (2021) 033 [[arXiv:2009.06668](#)] [[INSPIRE](#)].
- [82] A. Falkowski, G. Grilli di Cortona and Z. Tabrizi, *Future DUNE constraints on EFT*, *JHEP* **04** (2018) 101 [[arXiv:1802.08296](#)] [[INSPIRE](#)].

- [83] S. Pandey, S. Karmakar and S. Rakshit, *Strong constraints on non-standard neutrino interactions: LHC vs. IceCube*, *JHEP* **11** (2019) 046 [[arXiv:1907.07700](#)] [[INSPIRE](#)].
- [84] K.N. Deepthi, S. Goswami and N. Nath, *Can nonstandard interactions jeopardize the hierarchy sensitivity of DUNE?*, *Phys. Rev. D* **96** (2017) 075023 [[arXiv:1612.00784](#)] [[INSPIRE](#)].
- [85] K.N. Deepthi, S. Goswami and N. Nath, *Challenges posed by non-standard neutrino interactions in the determination of δ_{CP} at DUNE*, *Nucl. Phys. B* **936** (2018) 91 [[arXiv:1711.04840](#)] [[INSPIRE](#)].
- [86] J. Barranco, O.G. Miranda, C.A. Moura and J.W.F. Valle, *Constraining non-standard interactions in $\nu_e e$ or $\bar{\nu}_e e$ scattering*, *Phys. Rev. D* **73** (2006) 113001 [[hep-ph/0512195](#)] [[INSPIRE](#)].
- [87] J. Barranco, O.G. Miranda, C.A. Moura and J.W.F. Valle, *Constraining non-standard neutrino-electron interactions*, *Phys. Rev. D* **77** (2008) 093014 [[arXiv:0711.0698](#)] [[INSPIRE](#)].
- [88] A. Bolanos, O.G. Miranda, A. Palazzo, M.A. Tortola and J.W.F. Valle, *Probing non-standard neutrino-electron interactions with solar and reactor neutrinos*, *Phys. Rev. D* **79** (2009) 113012 [[arXiv:0812.4417](#)] [[INSPIRE](#)].
- [89] M. Lei, N. Steinberg and J.D. Wells, *Probing non-standard neutrino interactions with supernova neutrinos at Hyper-K*, *JHEP* **01** (2020) 179 [[arXiv:1907.01059](#)] [[INSPIRE](#)].
- [90] A. Esmaili and A.Y. Smirnov, *Probing non-standard interaction of neutrinos with IceCube and DeepCore*, *JHEP* **06** (2013) 026 [[arXiv:1304.1042](#)] [[INSPIRE](#)].
- [91] A. Friedland, C. Lunardini and M. Maltoni, *Atmospheric neutrinos as probes of neutrino-matter interactions*, *Phys. Rev. D* **70** (2004) 111301 [[hep-ph/0408264](#)] [[INSPIRE](#)].
- [92] A. Friedland and C. Lunardini, *A test of tau neutrino interactions with atmospheric neutrinos and K2K*, *Phys. Rev. D* **72** (2005) 053009 [[hep-ph/0506143](#)] [[INSPIRE](#)].
- [93] A.N. Khan and D.W. McKay, *$\sin^2(\theta)w$ estimate and bounds on nonstandard interactions at source and detector in the solar neutrino low-energy regime*, *JHEP* **07** (2017) 143 [[arXiv:1704.06222](#)] [[INSPIRE](#)].
- [94] C. Biggio, M. Blennow and E. Fernandez-Martinez, *Loop bounds on non-standard neutrino interactions*, *JHEP* **03** (2009) 139 [[arXiv:0902.0607](#)] [[INSPIRE](#)].
- [95] O. Tomalak, P. Machado, V. Pandey and R. Plestid, *Flavor-dependent radiative corrections in coherent elastic neutrino-nucleus scattering*, *JHEP* **02** (2021) 097 [[arXiv:2011.05960](#)] [[INSPIRE](#)].
- [96] P.B. Denton and J. Gehrlein, *A statistical analysis of the COHERENT data and applications to new physics*, [arXiv:2008.06062](#) [[INSPIRE](#)].
- [97] M. Hoferichter, J. Menéndez and A. Schwenk, *Coherent elastic neutrino-nucleus scattering: EFT analysis and nuclear responses*, *Phys. Rev. D* **102** (2020) 074018 [[arXiv:2007.08529](#)] [[INSPIRE](#)].
- [98] COHERENT collaboration, *Observation of coherent elastic neutrino-nucleus scattering*, *Science* **357** (2017) 1123 [[arXiv:1708.01294](#)] [[INSPIRE](#)].

- [99] O.G. Miranda, G. Sanchez Garcia and O. Sanders, *Coherent elastic neutrino-nucleus scattering as a precision test for the Standard Model and beyond: the COHERENT proposal case*, *Adv. High Energy Phys.* **2019** (2019) 3902819 [[arXiv:1902.09036](#)] [[INSPIRE](#)].
- [100] TEXONO collaboration, *Constraints on non-standard neutrino interactions and unparticle physics with neutrino-electron scattering at the Kuo-Sheng nuclear power reactor*, *Phys. Rev. D* **82** (2010) 033004 [[arXiv:1006.1947](#)] [[INSPIRE](#)].
- [101] A.N. Khan, *Global analysis of the source and detector nonstandard interactions using the short baseline $\nu - e$ and $\bar{\nu} - e$ scattering data*, *Phys. Rev. D* **93** (2016) 093019 [[arXiv:1605.09284](#)] [[INSPIRE](#)].
- [102] A. Ismail, R. Mammen Abraham and F. Kling, *Neutral current neutrino interactions at FASER ν* , *Phys. Rev. D* **103** (2021) 056014 [[arXiv:2012.10500](#)] [[INSPIRE](#)].
- [103] MOLLER collaboration, *The MOLLER experiment: an ultra-precise measurement of the weak mixing angle using Møller scattering*, [arXiv:1411.4088](#) [[INSPIRE](#)].
- [104] N. Berger et al., *Measuring the weak mixing angle with the P2 experiment at MESA*, *J. Univ. Sci. Tech. China* **46** (2016) 481 [[arXiv:1511.03934](#)] [[INSPIRE](#)].
- [105] Y. Du, A. Freitas, H.H. Patel and M.J. Ramsey-Musolf, *Parity-violating Møller scattering at next-to-next-to-leading order: closed fermion loops*, *Phys. Rev. Lett.* **126** (2021) 131801 [[arXiv:1912.08220](#)] [[INSPIRE](#)].
- [106] I. Esteban, M.C. Gonzalez-Garcia, M. Maltoni, I. Martinez-Soler and J. Salvado, *Updated constraints on non-standard interactions from global analysis of oscillation data*, *JHEP* **08** (2018) 180 [*Addendum ibid.* **12** (2020) 152] [[arXiv:1805.04530](#)] [[INSPIRE](#)].
- [107] Y. Farzan, M. Lindner, W. Rodejohann and X.-J. Xu, *Probing neutrino coupling to a light scalar with coherent neutrino scattering*, *JHEP* **05** (2018) 066 [[arXiv:1802.05171](#)] [[INSPIRE](#)].
- [108] J. Billard, J. Johnston and B.J. Kavanagh, *Prospects for exploring new physics in coherent elastic neutrino-nucleus scattering*, *JCAP* **11** (2018) 016 [[arXiv:1805.01798](#)] [[INSPIRE](#)].
- [109] D. Aristizabal Sierra, V. De Romeri and N. Rojas, *COHERENT analysis of neutrino generalized interactions*, *Phys. Rev. D* **98** (2018) 075018 [[arXiv:1806.07424](#)] [[INSPIRE](#)].
- [110] D.K. Papoulias and T.S. Kosmas, *COHERENT constraints to conventional and exotic neutrino physics*, *Phys. Rev. D* **97** (2018) 033003 [[arXiv:1711.09773](#)] [[INSPIRE](#)].
- [111] J.B. Dent, B. Dutta, S. Liao, J.L. Newstead, L.E. Strigari and J.W. Walker, *Accelerator and reactor complementarity in coherent neutrino-nucleus scattering*, *Phys. Rev. D* **97** (2018) 035009 [[arXiv:1711.03521](#)] [[INSPIRE](#)].
- [112] J. Liao and D. Marfatia, *COHERENT constraints on nonstandard neutrino interactions*, *Phys. Lett. B* **775** (2017) 54 [[arXiv:1708.04255](#)] [[INSPIRE](#)].
- [113] ALEPH, DELPHI, L3, OPAL, SLD, LEP ELECTROWEAK WORKING GROUP, SLD ELECTROWEAK GROUP and SLD HEAVY FLAVOUR GROUP collaborations, *Precision electroweak measurements on the Z resonance*, *Phys. Rept.* **427** (2006) 257 [[hep-ex/0509008](#)] [[INSPIRE](#)].
- [114] PLANCK collaboration, *Planck 2018 results. VI. Cosmological parameters*, *Astron. Astrophys.* **641** (2020) A6 [[arXiv:1807.06209](#)] [[INSPIRE](#)].

- [115] SPT-3G collaboration, *SPT-3G: a next-generation cosmic microwave background polarization experiment on the South Pole Telescope*, *Proc. SPIE Int. Soc. Opt. Eng.* **9153** (2014) 91531P [[arXiv:1407.2973](#)] [[INSPIRE](#)].
- [116] SIMONS OBSERVATORY collaboration, *The Simons Observatory: science goals and forecasts*, *JCAP* **02** (2019) 056 [[arXiv:1808.07445](#)] [[INSPIRE](#)].
- [117] CMB-S4 collaboration, *CMB-S4 science book, first edition*, [arXiv:1610.02743](#) [[INSPIRE](#)].
- [118] CORE collaboration, *Exploring cosmic origins with CORE: cosmological parameters*, *JCAP* **04** (2018) 017 [[arXiv:1612.00021](#)] [[INSPIRE](#)].
- [119] NASA PICO collaboration, *PICO: Probe of Inflation and Cosmic Origins*, [arXiv:1902.10541](#) [[INSPIRE](#)].
- [120] N. Sehgal et al., *CMB-HD: an ultra-deep, high-resolution millimeter-wave survey over half the sky*, [arXiv:1906.10134](#) [[INSPIRE](#)].
- [121] J.J. Bennett, G. Buldgen, M. Drewes and Y.Y.Y. Wong, *Towards a precision calculation of the effective number of neutrinos N_{eff} in the Standard Model I: the QED equation of state*, *JCAP* **03** (2020) 003 [*Addendum ibid.* **03** (2021) A01] [[arXiv:1911.04504](#)] [[INSPIRE](#)].
- [122] J.J. Bennett et al., *Towards a precision calculation of N_{eff} in the Standard Model II: neutrino decoupling in the presence of flavour oscillations and finite-temperature QED*, [arXiv:2012.02726](#) [[INSPIRE](#)].
- [123] K. Akita and M. Yamaguchi, *A precision calculation of relic neutrino decoupling*, *JCAP* **08** (2020) 012 [[arXiv:2005.07047](#)] [[INSPIRE](#)].
- [124] M. Escudero, *Neutrino decoupling beyond the Standard Model: CMB constraints on the dark matter mass with a fast and precise N_{eff} evaluation*, *JCAP* **02** (2019) 007 [[arXiv:1812.05605](#)] [[INSPIRE](#)].
- [125] M. Escudero Abenza, *Precision early universe thermodynamics made simple: N_{eff} and neutrino decoupling in the Standard Model and beyond*, *JCAP* **05** (2020) 048 [[arXiv:2001.04466](#)] [[INSPIRE](#)].
- [126] X. Luo, W. Rodejohann and X.-J. Xu, *Dirac neutrinos and N_{eff}* , *JCAP* **06** (2020) 058 [[arXiv:2005.01629](#)] [[INSPIRE](#)].
- [127] X. Luo, W. Rodejohann and X.-J. Xu, *Dirac neutrinos and N_{eff} . Part II. The freeze-in case*, *JCAP* **03** (2021) 082 [[arXiv:2011.13059](#)] [[INSPIRE](#)].
- [128] K.J. Kelly, M. Sen and Y. Zhang, *Intimate relationship between sterile neutrino dark matter and ΔN_{eff}* , [arXiv:2011.02487](#) [[INSPIRE](#)].
- [129] P. Adshead, Y. Cui, A.J. Long and M. Shamma, *Unraveling the Dirac neutrino with cosmological and terrestrial detectors*, [arXiv:2009.07852](#) [[INSPIRE](#)].
- [130] J.-T. Li, G.M. Fuller and E. Grohs, *Probing dark photons in the early universe with big bang nucleosynthesis*, *JCAP* **12** (2020) 049 [[arXiv:2009.14325](#)] [[INSPIRE](#)].
- [131] J. Venzor, A. Pérez-Lorenzana and J. De-Santiago, *Bounds on neutrino-scalar nonstandard interactions from big bang nucleosynthesis*, *Phys. Rev. D* **103** (2021) 043534 [[arXiv:2009.08104](#)] [[INSPIRE](#)].
- [132] J. Froustey, C. Pitrou and M.C. Volpe, *Neutrino decoupling including flavour oscillations and primordial nucleosynthesis*, *JCAP* **12** (2020) 015 [[arXiv:2008.01074](#)] [[INSPIRE](#)].

- [133] M. Ibe, S. Kobayashi, Y. Nakayama and S. Shirai, *Cosmological constraint on vector mediator of neutrino-electron interaction in light of XENON1T excess*, *JHEP* **12** (2020) 004 [[arXiv:2007.16105](#)] [[INSPIRE](#)].
- [134] XENON collaboration, *Excess electronic recoil events in XENON1T*, *Phys. Rev. D* **102** (2020) 072004 [[arXiv:2006.09721](#)] [[INSPIRE](#)].
- [135] V.F. Shvartsman, *Density of relict particles with zero rest mass in the universe*, *Pisma Zh. Eksp. Teor. Fiz.* **9** (1969) 315 [*JETP Lett.* **9** (1969) 184] [[INSPIRE](#)].
- [136] G. Steigman, D.N. Schramm and J.E. Gunn, *Cosmological limits to the number of massive leptons*, *Phys. Lett. B* **66** (1977) 202 [[INSPIRE](#)].
- [137] G. Mangano, G. Miele, S. Pastor and M. Peloso, *A precision calculation of the effective number of cosmological neutrinos*, *Phys. Lett. B* **534** (2002) 8 [[astro-ph/0111408](#)] [[INSPIRE](#)].
- [138] E.W. Kolb and M.S. Turner, *The early universe*, *Front. Phys.* **69** (1990) 1 [[INSPIRE](#)].
- [139] P.F. de Salas and S. Pastor, *Relic neutrino decoupling with flavour oscillations revisited*, *JCAP* **07** (2016) 051 [[arXiv:1606.06986](#)] [[INSPIRE](#)].
- [140] G. Mangano, G. Miele, S. Pastor, T. Pinto, O. Pisanti and P.D. Serpico, *Relic neutrino decoupling including flavor oscillations*, *Nucl. Phys. B* **729** (2005) 221 [[hep-ph/0506164](#)] [[INSPIRE](#)].
- [141] S. Hannestad, *Oscillation effects on neutrino decoupling in the early universe*, *Phys. Rev. D* **65** (2002) 083006 [[astro-ph/0111423](#)] [[INSPIRE](#)].
- [142] A.D. Dolgov, S.H. Hansen, S. Pastor, S.T. Petcov, G.G. Raffelt and D.V. Semikoz, *Cosmological bounds on neutrino degeneracy improved by flavor oscillations*, *Nucl. Phys. B* **632** (2002) 363 [[hep-ph/0201287](#)] [[INSPIRE](#)].
- [143] K. Abazajian et al., *CMB-S4 decadal survey APC white paper*, *Bull. Am. Astron. Soc.* **51** (2019) 209 [[arXiv:1908.01062](#)] [[INSPIRE](#)].
- [144] CMB-S4 collaboration, *CMB-S4 technology book, first edition*, [arXiv:1706.02464](#) [[INSPIRE](#)].
- [145] K.N. Abazajian et al., *Neutrino physics from the cosmic microwave background and large scale structure*, *Astropart. Phys.* **63** (2015) 66 [[arXiv:1309.5383](#)] [[INSPIRE](#)].
- [146] K. Abazajian et al., *CMB-S4 science case, reference design, and project plan*, [arXiv:1907.04473](#) [[INSPIRE](#)].
- [147] A.F. Heckler, *Astrophysical applications of quantum corrections to the equation of state of a plasma*, *Phys. Rev. D* **49** (1994) 611 [[INSPIRE](#)].
- [148] N. Fornengo, C.W. Kim and J. Song, *Finite temperature effects on the neutrino decoupling in the early universe*, *Phys. Rev. D* **56** (1997) 5123 [[hep-ph/9702324](#)] [[INSPIRE](#)].
- [149] S. Gariazzo, P.F. de Salas and S. Pastor, *Thermalisation of sterile neutrinos in the early universe in the 3 + 1 scheme with full mixing matrix*, *JCAP* **07** (2019) 014 [[arXiv:1905.11290](#)] [[INSPIRE](#)].
- [150] S. Hannestad and J. Madsen, *Neutrino decoupling in the early universe*, *Phys. Rev. D* **52** (1995) 1764 [[astro-ph/9506015](#)] [[INSPIRE](#)].

- [151] A.D. Dolgov, S.H. Hansen and D.V. Semikoz, *Nonequilibrium corrections to the spectra of massless neutrinos in the early universe*, *Nucl. Phys. B* **503** (1997) 426 [[hep-ph/9703315](#)] [[INSPIRE](#)].
- [152] A.D. Dolgov, S.H. Hansen and D.V. Semikoz, *Nonequilibrium corrections to the spectra of massless neutrinos in the early universe: addendum*, *Nucl. Phys. B* **543** (1999) 269 [[hep-ph/9805467](#)] [[INSPIRE](#)].
- [153] J. Birrell, C.-T. Yang and J. Rafelski, *Relic neutrino freeze-out: dependence on natural constants*, *Nucl. Phys. B* **890** (2014) 481 [[arXiv:1406.1759](#)] [[INSPIRE](#)].
- [154] I.M. Oldengott, T. Tram, C. Rampf and Y.Y.Y. Wong, *Interacting neutrinos in cosmology: exact description and constraints*, *JCAP* **11** (2017) 027 [[arXiv:1706.02123](#)] [[INSPIRE](#)].
- [155] I.M. Oldengott, C. Rampf and Y.Y.Y. Wong, *Boltzmann hierarchy for interacting neutrinos I: formalism*, *JCAP* **04** (2015) 016 [[arXiv:1409.1577](#)] [[INSPIRE](#)].
- [156] E. Grohs, G.M. Fuller, C.T. Kishimoto, M.W. Paris and A. Vlasenko, *Neutrino energy transport in weak decoupling and big bang nucleosynthesis*, *Phys. Rev. D* **93** (2016) 083522 [[arXiv:1512.02205](#)] [[INSPIRE](#)].
- [157] R. Yunis, C.R. Argüelles and D. López Nacir, *Boltzmann hierarchies for self-interacting warm dark matter scenarios*, *JCAP* **09** (2020) 041 [[arXiv:2002.05778](#)] [[INSPIRE](#)].
- [158] C.D. Kreisch, F.-Y. Cyr-Racine and O. Doré, *Neutrino puzzle: anomalies, interactions, and cosmological tensions*, *Phys. Rev. D* **101** (2020) 123505 [[arXiv:1902.00534](#)] [[INSPIRE](#)].
- [159] S. Esposito, G. Miele, S. Pastor, M. Peloso and O. Pisanti, *Nonequilibrium spectra of degenerate relic neutrinos*, *Nucl. Phys. B* **590** (2000) 539 [[astro-ph/0005573](#)] [[INSPIRE](#)].
- [160] J. Froustey and C. Pitrou, *Incomplete neutrino decoupling effect on big bang nucleosynthesis*, *Phys. Rev. D* **101** (2020) 043524 [[arXiv:1912.09378](#)] [[INSPIRE](#)].
- [161] A. Fradette, M. Pospelov, J. Pradler and A. Ritz, *Cosmological beam dump: constraints on dark scalars mixed with the Higgs boson*, *Phys. Rev. D* **99** (2019) 075004 [[arXiv:1812.07585](#)] [[INSPIRE](#)].
- [162] T. Kinoshita, *Mass singularities of Feynman amplitudes*, *J. Math. Phys.* **3** (1962) 650 [[INSPIRE](#)].
- [163] T.D. Lee and M. Nauenberg, *Degenerate systems and mass singularities*, *Phys. Rev.* **133** (1964) B1549 [[INSPIRE](#)].
- [164] C. Frye, H. Hannesdottir, N. Paul, M.D. Schwartz and K. Yan, *Infrared finiteness and forward scattering*, *Phys. Rev. D* **99** (2019) 056015 [[arXiv:1810.10022](#)] [[INSPIRE](#)].
- [165] CMS collaboration, *Observation of a new boson at a mass of 125 GeV with the CMS experiment at the LHC*, *Phys. Lett. B* **716** (2012) 30 [[arXiv:1207.7235](#)] [[INSPIRE](#)].
- [166] A.G. Riess, S. Casertano, W. Yuan, L.M. Macri and D. Scolnic, *Large Magellanic cloud cepheid standards provide a 1% foundation for the determination of the Hubble constant and stronger evidence for physics beyond Λ CDM*, *Astrophys. J.* **876** (2019) 85 [[arXiv:1903.07603](#)] [[INSPIRE](#)].
- [167] T. Brinckmann, J.H. Chang and M. LoVerde, *Self-interacting neutrinos, the Hubble parameter tension, and the cosmic microwave background*, [arXiv:2012.11830](#) [[INSPIRE](#)].

- [168] S. Roy Choudhury, S. Hannestad and T. Tram, *Updated constraints on massive neutrino self-interactions from cosmology in light of the H_0 tension*, *JCAP* **03** (2021) 084 [[arXiv:2012.07519](#)] [[INSPIRE](#)].
- [169] A. Das and S. Ghosh, *Flavor-specific interaction favors strong neutrino self-coupling in the early universe*, [arXiv:2011.12315](#) [[INSPIRE](#)].
- [170] G.-Y. Huang and W. Rodejohann, *Solving the Hubble tension without spoiling big bang nucleosynthesis*, [arXiv:2102.04280](#) [[INSPIRE](#)].
- [171] BOREXINO collaboration, *Limiting neutrino magnetic moments with Borexino phase-II solar neutrino data*, *Phys. Rev. D* **96** (2017) 091103 [[arXiv:1707.09355](#)] [[INSPIRE](#)].
- [172] H.H. Patel, *Package-X 2.0: a Mathematica package for the analytic calculation of one-loop integrals*, *Comput. Phys. Commun.* **218** (2017) 66 [[arXiv:1612.00009](#)] [[INSPIRE](#)].
- [173] A.D. Dolgov, *Neutrinos in cosmology*, *Phys. Rept.* **370** (2002) 333 [[hep-ph/0202122](#)] [[INSPIRE](#)].